Journal of Nuclear Medicine, published on November 22, 2019 as doi:10.2967/jnumed.119.232934

Imaging DNA Damage Repair *in vivo* Following ^{177}Lu-DOTATATE Therapy

Edward O'Neill[1], Veerle Kersemans[1], P. Danny Allen[1], Samantha Y.A. Terry[2], Julia Baguña Torres[1], Michael Mosley[1], Sean Smart[1], Boon Quan Lee[1], Nadia Falzone[1], Katherine A. Vallis[1], Mark W. Konijnenberg[3], Marion de Jong[3], Julie Nonnekens[3,4,5], Bart Cornelissen[1,*]

[1] CRUK/MRC Oxford Institute for Radiation Oncology, Department of Oncology, University of Oxford, Oxford, UK
[2] Department of Imaging Chemistry and Biology, King's College London, London, UK
[3] Department of Radiology and Nuclear Medicine, Erasmus MC, Rotterdam, The Netherlands
[4] Department of Molecular Genetics, Erasmus MC, Rotterdam, The Netherlands
[5] Oncode Institute, Erasmus MC, Rotterdam, The Netherlands

Word count: 4,648
Running Title: Imaging γH2AX after 177Lu PRRT
Key words: ^{177}Lu-DOTATATE; γH2AX; SPECT; DNA damage; neuroendocrine cancer
Financial Support: EON, NF, KV, SYAT, JN, MdJ, and BC were supported by MRC (MR/P018661/1). BC, MM, SS, PDA, and VK were supported by CRUK through the CRUK/MRC Oxford Institute for Radiation Oncology. JBT was supported by PCRF. SYAT was also supported by the Academy of Medical Sciences [SBF001\1019] and the Wellcome/EPSRC Centre for Medical Engineering at King's College London [WT 203148/Z/16/Z]. JN was also supported by the Daniel den Hoed Foundation.
Disclosure: JN and MdJ have received financial support for research projects from AAA. No other potential conflicts of interest relevant to this article exist.

* **To whom correspondence should be addressed:**
Professor Bart Cornelissen
CRUK/MRC Oxford Institute for Radiation Oncology
Department of Oncology
University of Oxford
Old Road Campus Research Building
Off Roosevelt Drive
Oxford OX3 7LJ
Tel: +44 (0)1865 857126
Fax: +44 (0)1865 857127
Email: bart.cornelissen@oncology.ox.ac.uk

First author
Dr Edward O'Neill
CRUK/MRC Oxford Institute for Radiation Oncology
Department of Oncology
University of Oxford
Old Road Campus Research Building
Off Roosevelt Drive
Oxford OX3 7LJ
Tel: +44 (0)1865 857126
Fax: +44 (0)1865 857127
Email: edward.oneill@oncology.ox.ac.uk

ABSTRACT

Purpose. Molecular Radiotherapy (MRT) using ^{177}Lu-DOTATATE is a most effective therapy for the treatment of somatostatin receptor expressing neuroendocrine tumors (NETs). Despite its frequent and successful use in the clinic, little or no radiobiological considerations are taken into account at the time of treatment planning or delivery, and upon positive uptake of octreotide-based PET/SPECT imaging, treatment is usually administered as a standard dose and number of cycles without adjustment for peptide uptake, dosimetry, or radiobiological and DNA damage effects in the tumor. Here, we visualize and quantify the extent of DNA damage response following ^{177}Lu-DOTATATE therapy using SPECT imaging with ^{111}In-anti-γH2AX-TAT. This work is a proof-of-principle study of this *in vivo* non-invasive biodosimeter with beta-emitting therapeutic radiopharmaceuticals.

Methods. Six cell lines were exposed to external beam radiotherapy (EBRT) or ^{177}Lu-DOTATATE, after which the number of γH2AX foci and clonogenic survival were measured. Mice bearing CA20948 somatostatin receptor positive tumor xenografts were treated with ^{177}Lu-DOTATATE or sham-treated, and co-injected with ^{111}In-anti-γH2AX-TAT, ^{111}In-IgG-TAT control, or vehicle.

Results. Clonogenic survival following EBRT was cell line specific, indicating varying levels of intrinsic radiosensitivity. *In vitro*, cell lines treated with ^{177}Lu-DOTATATE, clonogenic survival decreased and γH2AX foci increased in cells expressing high levels of somatostatin receptor subtype 2 (SST2). *Ex vivo* measurements revealed a partial correlation between ^{177}Lu-DOTATATE uptake and γH2AX foci induction between different regions of CA20948 xenograft tumors, suggesting different parts of the tumor may react differentially to ^{177}Lu-DOTATATE irradiation.

Conclusion. ^{111}In-anti-γH2AX-TAT allows monitoring of DNA damage following ^{177}Lu-DOTATATE therapy, and reveals heterogeneous damage responses.

INTRODUCTION

Neuroendocrine tumors (NETs) comprise a heterogeneous group of neoplasms derived from peptide- and amine-producing cells of the neuroendocrine system. Despite their relatively low incidence, NETs are a heterogeneous and complicated tumor family and represent a significant clinical challenge requiring multidisciplinary care (*1*). Somatostatin receptor (SST2 or 5) expression in most differentiated neuroendocrine cancers allows treatment with somatostatin analogues such as octreotide, as well as imaging and therapy with radiolabelled somatostatin analogues. Compounds such as DOTATOC ((DOTA^0-Tyr^3)octreotide) or DOTATATE ((DOTA^0-Tyr^3)-octreotate), are radiolabeled with gamma-emitting radionuclides such as ^{111}In for SPECT imaging, positron emitters such as ^{68}Ga for PET imaging, or the beta-emitting ^{177}Lu or ^{90}Y for Molecular Radiotherapy (MRT). MRT with small radiolabelled peptides, also called Peptide Receptor Radionuclide Therapy (PRRT), using these beta-emitting radiopharmaceuticals is now used routinely to treat NET patients (*2*). A large phase 3 study (the NETTER trial) demonstrated that ^{177}Lu-DOTATATE significantly improved progression-free survival when compared with high-dose octreotide in patients with advanced midgut neuroendocrine tumors, with minimal and transient side effects (*3,4*).

The radiobiological aspects of ^{177}Lu-DOTATATE, as for other MRT radiopharmaceuticals, have been underexplored (*5*). Despite its frequent and successful use, dosimetry is not always taken into account at the time of PRRT treatment planning or delivery, and little radiobiological evaluation is performed (*6,7*), and therapy outcome is not measured until late (3 months) after treatment, with no measurements of intratumoral heterogeneity, intracellular dosimetry, or short- term efficacy readouts.. Although ^{177}Lu-DOTATATE, ^{90}Y-DOTATOC – and, increasingly, ^{177}Lu-PSMA (Prostate Specific Membrane Antigen) – are widely used throughout Europe, therapy invariably consists of 2 or 4 intravenous administrations of 7.4 GBq, separated by nine to twelve weeks, mostly regardless of the patient's size, weight, the extent of positive ^{111}In-octreotide or ^{68}Ga-DOTATATE uptake (measured by SPECT or PET imaging, respectively), or inherent radiosensitivity of the tumor or patient (*8,9*). Importantly, most MRT dosimetry and radiobiology has been based on EBRT data, due to a paucity in radiobiological data of radionuclide therapy (*10*). This substitution of EBRT for MRT dosimetry cannot adequately account for the distinct and complex cellular localization of ionising radiation with MRT, and the distinctly different dynamic biological response across the timeframe of exposure during MRT. Although *in vitro* dosimetry methods exist, they require optimization for each cell line, and progressively complicated for each cell line with *in vitro* 3D spheroid cellular constructs (*11*). Even despite the best assessments of physical dose

deposition, the effect that matters most is radiation cytotoxicity, and different cells, including cancer cells, react differently to the same absorbed dose. Thus, a 'biological' dosimetry approach may be used, by measuring the extent of biological response to ionising radiation, such as DNA damage repair signalling. This biodosimetry approach could be considered a more direct measure of effective biological dose, and may have greater translational potential in the clinic.

The major cytotoxic effect of MRT is mediated by causing DNA damage. The beta decay of ^{177}Lu-DOTATATE induces a variety of DNA damage, including single strand breaks, as well as DNA double strand break damage, one of the most lethal types of DNA damage. One of the responses to DNA double strand break damage, is phosphorylation of the histone isoform H2AX on serine-139 to form γH2AX. This is expressed in foci of several thousand copies around the DNA double strand break site, where it acts as a scaffold to attract downstream DNA repair factors. γH2AX repair foci have traditionally been used in radiobiology to gauge the extent of DNA double strand break damage following ionising radiation, such as EBRT.

Previously, we have developed a radiolabelled modified version of an anti- γH2AX antibody, ^{111}In-anti-γH2AX-TAT, that allows to non-invasively visualize and quantify γH2AX expression in tumor tissue, as a surrogate imaging-based measure of the extent of DNA double strand break damage. The radiolabelled full-length antibody is modified with the TAT-peptide, a cell penetrating peptide that incorporates a nuclear localization sequence, to enable the antibody to enter cells and penetrate to the nucleus, to access its exclusively intranuclear target, γH2AX (*12*). We showed that ^{111}In-anti- γH2AX-TAT, using SPECT imaging, enables to measure DNA damage after EBRT (*13-15*), EBRT plus a radiosensitizer, such as an ATR inhibitor (*16*), chemotherapies such as bleomycin, 5-FU, gemcitabine or capecitabine in mouse models of breast or pancreatic cancer (*13,17*), or DNA damage repair hyperactivation during tumorigenesis in a mouse model of HER2-driven breast cancer (*12,18*), reviewed in (*13*). In addition, we reported on a ^{89}Zr-labelled version for PET imaging of γH2AX, for PET imaging (*15*).

Apart from beta-particles, ^{177}Lu emits gamma-rays (113 and 208 keV), that can be used for SPECT imaging. This can be used to determine the accumulation of ^{177}Lu in tissue, and calculate radiation absorbed dose. The gamma emissions of ^{111}In do not overlap with ^{177}Lu (171 and 245 keV), allowing dual isotope imaging to assess, at the same time, the physical dose distribution of ^{177}Lu, as well as its biological effect on DNA damage repair signalling, with ^{111}In-anti-γH2AX-TAT. This method may, therefore, allow adaptive clinical treatment regimes.

Here, we demonstrate that ^{177}Lu-DOTATATE therapy results in the formation of γH2AX foci in a mouse model of neuroendocrine cancer, allowing us to gauge the extent of DNA damage using the *in vivo* biodosimeter, ^{111}In-anti-γH2AX-TAT, using dual isotope SPECT imaging of ^{177}Lu and ^{111}In.

MATERIALS AND METHODS

Full materials and methods are presented in the supplementary material accompanying this manuscript.

General

^{177}Lu-DOTATATE was prepared using previously described methods (*19*). Carrier-free ^{177}Lu was obtained from ITG (Germany), DOTATATE precursor was obtained from Cambridge Biosciences. ^{177}Lu-DOTATATE was prepared to a molar activity of 50 MBq/nmol for *in vitro* use, and 86 MBq/nmol (60 MBq/μg) for *in vivo* experiments, unless otherwise stated. Radiolabeling yield was routinely >99.5%, as determined by ITLC. Immunoconjugate preparation and radiosynthesis of ^{111}In-anti-γH2AX-TAT and ^{111}In-IgG-TAT was performed using mouse monoclonal anti-γH2AX antibodies (Merck, clone JBW-301) or isotype-matched mouse non-specific antibodies, as previously described (*13*).

Cells, Cell Uptake and Fractionation

Cell membrane-association, internalization and nuclear localization of ^{177}Lu-DOTATATE were studied in CA20948, BON1, QGP1, H727, U2OS and U2OS^{SSTR2} cell lines. We used the rat pancreatic cancer cell line CA20948 for our most of the work described below, including *in vivo* studies, since it is one of only a handful of pancreatic cancer models described in the literature that mimic the SST-overexpression found in many human neuroendocrine tumors, and form tumors *in vivo*. The cell line was derived from a rat pancreas, and is acinar in origin, yet displays a neuroendocrine phenotype. Cells were harvested using Accutase (Biolegend). Aliquots of 2×10^5 cells in 200 μL of growth medium were exposed to ^{177}Lu-DOTATATE (2.5 MBq/mL, 50 MBq/nmol) for increasing amounts of time at 37°C for up to 24 h. The amount of ^{177}Lu associated with cell membrane, cytoplasm and nucleus was then measured using an automated gamma counter following cell fractionation as previously described (*20*).

Clonogenic Survival

Cell suspensions (0.2×10^5 cells) were prepared using Accutase, resuspended in growth media (200 μL) and treated with either radiolabeled ^{177}Lu-DOTATATE (0-2.5 MBq/mL, 50 MBq/nmol) and

incubated at 37°C for 2 h, or exposed to external gamma irradiation (0 - 10 Gy, 1 Gy/min, using a ^{137}Cs irradiator), or sham treated. An aliquot of cells for each treatment condition was plated in 6-well plates with 2 mL of growth media and incubated at 37°C in 5% CO_2. After 2 weeks, the number of colonies with more than 50 cells was counted to determine the clonogenic survival fraction. Geometries derived from confocal microscopy measurements of the dimensions of all cells in the panel allowed the calculation of S-values, which were used for micro-dosimetry of ^{177}Lu. The total radiation absorbed dose from ^{177}Lu to cell nuclei was determined using a MIRD-based approach, assuming homogeneous ^{177}Lu uptake on membrane, in cytoplasm, and in the nucleus. The total dose was calculated as the sum of self-dose and cross-dose.

γH2AX Imaging by Confocal Microscopy.

Cells were grown in 8-well culture chambers. After exposure of cells to ^{177}Lu-DOTATATE (2.5 MBq/mL, 50 MBq/nmol) for 2 h, or to external beam irradiation (6 Gy), they were left to recover in fresh growth medium for 1, 24, 48, or 72 h. Cells were then washed, fixed, permeabilized and stained using a mouse anti-γH2AX antibody (clone JBW-301, 1:800).

In Vivo Imaging.

All animal procedures were performed in accordance with the UK Animals (Scientific Procedures) Act 1986 and with local ethical committee approval. Female athymic nude mice were housed in IVC cages in groups of up to five per cage in an artificial day-night cycle facility with *ad libitum* access to food and water. Tumor xenografts were generated by subcutaneous injection of cell suspensions (10^6 cells in 100 µL serum-free growth medium) in the right hind flank. Static SPECT/CT images were acquired at 1, 24, 48 and 72 h after an intravenous bolus administration of ^{177}Lu-DOTATATE (20 MBq, 0.33 µg, in 100 µL phosphate buffered saline [PBS]). In a separate study, immediately after the 1 h SPECT image, mice were additionally administered intravenously a bolus injection of ^{111}In-anti-γH2AX-TAT, ^{111}In-IgG-TAT (5 MBq, 5 µg, in 100 µL PBS), or PBS control (Supplemental Fig. 1). The average tumor size at the start of the study was 177 ± 101 mm^3. The average weight of animals was 18 ± 1.1 g. SPECT/CT images were acquired in list-mode for approximately 10 minutes using a single gantry SPECT/PET/CT scanner (VECTor^{4}CT, MILabs, Utrecht, the Netherlands) equipped with the HE-UHR-RM collimator containing pinhole apertures of 1.8 mm diameter. Reconstructed images were viewed and analyzed using PMOD v.3.38 (PMOD Technologies, Zurich, Switzerland). Five animals were used per group. After the final imaging session, animals were culled, and

blood and selected tissues were harvested. ^{177}Lu quantification on SPECT images was based on analysis of a series of standards with known activity. Dual isotope image reconstruction and quantification was performed using a series of phantoms containing a range of ^{111}In:^{177}Lu mixtures (Supplemental Fig. 2). Digital autoradiography and immunofluorescence confocal microscopy staining for γH2AX was performed on 10 µm tumor sections. U2OS or U2OS^{sstr2} cells did not form xenografts in Balb/c nu/nu mice in our hands. Radiation absorbed dose from ^{177}Lu was calculated as previously described, based on volume-of-interest (VOI)-derived volume measurements (*3*). Calculations of the absorbed dose and absorbed dose rates at each time-point, using the spheres model features in the IDAC code for lymphoid tissue at 1.03 g/ml density.

Statistical Analysis.

All statistical and regression analyses were performed using GraphPad Prism v7 (GraphPad Software, San Diego, CA, USA). Linear regression with Runs test was used to check for correlations between measurements. After testing for normality using a Shapiro-Wilk test, means were compared using a t-test with Welch's correction for non-equal variances, where applicable. One-way ANOVA tests followed by Dunnet's post-tests were used to compare multiple groups. Two-way ANOVA tests were used to analyse grouped data. All results are reported as mean ± standard deviation of at least three independent replicates.

RESULTS

^{177}Lu-DOTATATE Exposure and External Beam Radiation Therapy Cause Differential Effects in a Set of Cell Lines in Vitro

Clonogenic survival after EBRT (0-10 Gy) in a panel of six cell lines revealed that all six lines present with inherently distinct radiation sensitivities (Fig. 1, Supplemental Fig 3, Supplemental Table 1), apart from the U2OS/U2OS^{sstr2} pair, where transfection of SST2 has no significant effect on clonogenic survival ($P>0.05$). D_{90} values (the radiation absorbed dose at which clonogenic survival has dropped 10-fold) are 5.3, 5.4, 5.5, 5.7, 8.0, and 9.5 Gy for U2OS, U2OS^{sstr2}, BON1, CA20984, H727, and QGP1 cells, respectively. This indicates that the various cells have varying levels of sensitivity to EBRT.

Uptake of ^{177}Lu-DOTATATE in a panel of six cancer cell lines *in vitro* occurred in line with expression or SST2 expression, and resulted in reduced clonogenic survival in cell lines expressing SST (Figs. 1-2, Supplemental Fig. 4). Transfection of SST-negative U2OS cells to stably express SST2 receptors

resulted in a 40-fold increase in cell-associated ^{177}Lu, after 2 h of exposure to ^{177}Lu- DOTATATE (6.2±1.7 vs. 250±1.6 mBq/cell; P<0.0001) (Supplemental Fig. 4). CA20948 cells, which naturally express high levels of SST2 receptors, when exposed to ^{177}Lu-DOTATATE, took up ^{177}Lu (57±5.0 mBq/cell), in contrast to QGP1, BON1, or H727 cells, which all express low levels of SST receptors (8.9±2.3, 6.2±5.4, and 8.4±1.1 mBq/cell, respectively). Not surprisingly, clonogenic survival was only reduced significantly in cells that express SST, and thus take up ^{177}Lu-DOTATATE.

The amount of ^{177}Lu associated with membrane, cytoplasm, and the nucleus of all cells at various times after exposure to ^{177}Lu-DOTATATE (Supplemental Fig. 4) was determined from cellular fractionation. Although most cell-associated ^{177}Lu was associated with the membrane at all time points, a significant amount was associated with the cytoplasmic fraction (13% in CA20948 cells at 2 h), but very little in the nucleus (<0.1%). Differences with previously reported results may be explained by the fact that here, we perform the measurements not on adherent cells, but on cells in suspension. Given the range of beta particles emitted by ^{177}Lu (on average 1.7 mm), this results in radiation dose to the cells and their nuclei, resulting in reduced clonogenic survival.

Within these monoclonal cell cultures, clonogenic survival of cells after exposure to ^{177}Lu-DOTATATE correlated well with absorbed dose (Fig. 1). However, comparing CA20948 and U2OS^{sstr2} cells, the same radiation absorbed dose from ^{177}Lu-DOTATATE resulted in different clonogenic survival, as compared to external beam radiation therapy (EBRT). Clonogenic survival was higher for EBRT in CA20948 cells compared to the same radiation dose of ^{177}Lu-DOTATATE (P<0.0001), whereas it was lower in U2OS^{sstr2} cells (P<0.0001) (Supplemental Table 1). This reinforces previous reports that the same dose of EBRT and MRT do not result in the same biological effect, and that this difference may be different in different cell lines (*21*).

^{177}Lu-DOTATATE Exposure in SST-positive Cells Results in γH2AX Foci in Vitro

Exposure of all cells to EBRT led to formation of γH2AX foci, to different extents in each cell type (Fig. 2a). In CA20498 cells, exposure to ^{177}Lu-DOTATATE for 2 h also resulted in DNA double strand break damage, as measured by γH2AX foci (Fig. 2B, C). Interestingly, the number of γH2AX foci continued to increase significantly up to 72 h following exposure to ^{177}Lu-DOTATATE (42 ± 14 foci/cell vs. 15 ± 9.7 foci/cell in treated vs. non-treated cells; P<0.0001). This was in stark contrast to the number of γH2AX foci following a single dose of EBRT, where γH2AX foci were high shortly after irradiation (67±18 foci/cell; P<0.0001), but soon retuned back to pre-treatment levels (13±6.1; P>0.05 at 72 h), as is

expected in most cells without DNA damage repair defects.

A similar result was obtained in U2OS^{sstr2} cells, although here the number of γH2AX foci did not increase at 72 h after exposure to ^{177}Lu-DOTATATE, but at all times was higher than the number of foci in wild type U2OS cells (P<0.0001; Supplemental Fig. 5). These results were in concordance with earlier results from Dalm et al., who showed the formation of another type of DNA damage repair foci, 53BP1 foci, after ^{177}Lu-DOTATATE treatment of U2OS^{sstr2} cells (*22,23*).

Thus, DNA damage repair signaling, as measured by γH2AX foci, following exposure ^{177}Lu-DOTATATE is distinct from that following EBRT.

^{177}Lu-DOTATATE Uptake in Xenograft Tumors Induces γH2AX Foci in Vivo

Intravenous administration of ^{177}Lu-DOTATATE to CA20948 tumor xenograft-bearing mice resulted in high tumor uptake (36 ± 4.5%ID/mL at 24 h after administration; Fig. 3A), whereas other xenografts took up far less ^{177}Lu-DOTATATE (P<0.0001), in line with *in vitro* results, and SST expression levels (Supplemental Fig. 6A). Dynamic SPECT imaging revealed maximum tumor uptake in CA20948 xenografts was reached at 60 min after administration (Supplemental Fig. 6B).

Comparable to our *in vitro* results described above, high ^{177}Lu-DOTATATE uptake and γH2AX foci formation was observed in CA20948 xenografts, 72 h after administration of ^{177}Lu-DOTATATE (Fig. 3B-F), compared to non-treated tumors (Fig. 3G). The delivery of ^{177}Lu-DOTATATE to the tumors was heterogeneously distributed, which has been observed previously (*24*). Comparison of autoradiography showing ^{177}Lu uptake in a tumor section with immunohistochemistry staining for γH2AX revealed that, in general, areas of tumor with higher ^{177}Lu uptake showed higher number of γH2AX foci per cell (Fig 3E) and areas with low ^{177}Lu uptake showed fewer γH2AX foci per cell (Fig 3F), but this correlation was not linear or significant. Only few cells with pan-nuclear staining, indicating late-stage apoptosis, were observed. Interestingly, a large number of intermediate ^{177}Lu uptake regions could also be observed, where the number of γH2AX foci was highly variable. A correlation plot comparing the two signals quantitatively revealed a similar lack of pattern (Fig 3D). Similar observations were made in all tumors (three additional examples are shown in Supplemental Fig. 7). This indicates that γH2AX may be used as a marker for the biological effect of ^{177}Lu therapy.

^{111}In-anti-γH2AX-TAT Allows in Vivo Imaging of DNA Damage after ^{177}Lu-DOTATATE Therapy

^{111}In-anti-γH2AX-TAT enabled imaging of γH2AX *in vivo*. Dual isotope imaging of ^{177}Lu-

DOTATATE and ^{111}In-anti-γH2AX-TAT allowed concurrent imaging of tumor-associated ^{177}Lu, and visualization of the DNA double strand break damage resulting from the emitted β-particles. The ability of the MILabs VECTor^4 imaging system to simultaneously acquire images for ^{111}In and ^{177}Lu was evaluated using phantoms containing mixtures of known amounts of either radionuclide. Samples containing ^{177}Lu only did not show any signal in the reconstructed ^{111}In image, or vice versa. Importantly, quantification of ^{111}In or ^{177}Lu was not influenced by the presence of the other isotope (R = 0.99, P < 0.0001; Supplemental Fig. 2), corroborating earlier reports on dual-isotope imaging with this system (*25,26*).

^{111}In-anti-γH2AX-TAT uptake increased in tumors treated with ^{177}Lu-DOTATATE. VOI analysis of the ^{111}In signal in SPECT/CT images acquired at various time points revealed a significant increase in tumor uptake of ^{111}In-anti-γH2AX-TAT in CA20948 tumor xenografts, 72 h after injection, 73 h after intravenous administration of 20 MBq ^{177}Lu-DOTATATE, as compared to ^{111}In-anti-γH2AX-TAT uptake in control animals (P=0.0033), or compared to uptake of the non-specific control compound, ^{111}In-IgG- TAT, with or without ^{177}Lu treatment (P<0.0001) (Figs. 4 and 5). Uptake of the non-specific control compound, ^{111}In-IgG-TAT, was not altered by treatment of the tumors with ^{177}Lu-DOTATATE (P = 0.41), confirming that the effect on ^{111}In-anti-γH2AX-TAT is not due to physiological changes that may affect non-specific uptake of the IgG-TAT construct. Detailed data on the tumor uptake in each mouse is reported in Supplemental Fig. 8. In addition, we observed no significant differences on the uptake of ^{177}Lu in tumors or any normal tissues after administration of ^{111}In-anti-γH2AX-TAT compared to ^{111}In- IgG-TAT (P>0.05) (Fig. 4B and Supplemental Fig. 9). *In vivo* tumor uptake of ^{111}In-anti-γH2AX-TAT followed the same trend over 72 h as the number of γH2AX foci *in vitro* after brief exposure to ^{177}Lu- DOTATATE.

No statistically significant differences in uptake of ^{111}In-anti-γH2AX-TAT or ^{111}In-IgG-TAT were observed in any of the organs in mice exposed to ^{177}Lu-DOTATATE versus untreated animals (P > 0.05), with the exception of the spleen (P = 0.0009) (Supplemental Fig. 9). Given the very low uptake of ^{177}Lu in the mouse spleen (0.43±0.23%ID/g at 72 h), radiation exposure seems an unlikely source in mouse, although in humans the spleen receives a non-negligible dose following ^{177}Lu-DOTATATE (4.5-15 Gy over 2-5 cycles) (*27*). Notably, in our experimental setup, we observed no differences in the uptake of ^{111}In-anti-γH2AX-TAT in the kidneys of the mice, the tissue that is exposed most to ^{177}Lu radiation dose, second only to the tumor.

VOI analysis of the ^{177}Lu signal in all images allowed to calculate the average radiation absorbed dose to the tumor in ^{177}Lu-DOTATATE -treated animals as 12.9 ± 3.4 Gy (after 72 h, Supplemental Table

2, Supplemental Fig. 10), similar to previously reported values (*23*). Clearance from the tumor xenografts occurred with a mean effective half-life of 46.3 ± 8.6 h. There was no statistical difference in the average absorbed dose from ^{177}Lu in animals imaged with ^{111}In-anti-γH2AX- TAT compared to ^{111}In-IgG-TAT (P = 0.15, Mann-Whitney test). Contrary to our earlier observations following EBRT (*13*), accumulated absorbed dose from ^{177}Lu, or the dose rate of ^{177}Lu at any given time, did not correlate with ^{111}In-anti-γH2AX-TAT uptake in the tumor, at least not in the limited dataset analyzed here (P > 0.55, n = 5).

^{111}In-anti-γH2AX-TAT Heterogeneity in vivo

Pixel-per-pixel segmentation of tumor volumes, based on the magnitude of the ^{177}Lu signal, allowed correlation with the amount of ^{111}In-signal, in various substructures within the tumor (Fig. 5). Consistent with our earlier *ex vivo* γH2AX foci measurements (Fig. 3), qualitative analysis revealed that, in general, areas within the tumor with higher ^{177}Lu uptake also took up more ^{111}In-anti-γH2AX- TAT at all time points, a correlation which was linear up to approximately 20%ID/g of ^{177}Lu (R^2 = 0.9843, P<0.0001, Fig 5B), but not ^{111}In-IgG-TAT (Fig. 5D). However, consistent with our abovementioned finding (Fig. 3), our results hint towards a more complex relationship between ^{177}Lu uptake and the radiobiological response, especially at the higher end of ^{177}Lu exposure, compared to what a ^{177}Lu- radiation deposited dose alone would suggest.

DISCUSSION

Here we show, for the first time, that it is possible to visualize and quantify the DNA double strand break damage marker γH2AX, as induced by molecular radiotherapy with ^{177}Lu, in a non- invasive manner, by whole-body molecular imaging. First, we confirm that exposure of SST-expressing cells to ^{177}Lu-DOTATATE *in vitro* resulted in reduced clonogenic survival. Different cell lines responded differently to the same ^{177}Lu absorbed dose. The same was true for EBRT. Nonetheless, sensitivity to EBRT did not correlate linearly with sensitivity to ^{177}Lu. DNA double strand break damage was observed *in vitro* by immunofluorescence, as measured by γH2AX foci. Kinetics of γH2AX formation and dissolution was different following ^{177}Lu exposure and EBRT. It has been shown previously that therapeutic success of ionizing radiation is closely correlated with the induction of DNA double strand break damage, especially with late, unrepaired damage (*28*). ^{177}Lu-DOTATATE causes DNA damage *in vivo* in tumor tissue, and thus causes expression of γH2AX. We demonstrate that this induction of γH2AX following ^{177}Lu-DOTATATE therapy can be monitored by SPECT imaging with ^{111}In-anti-γH2AX- TAT. This allowed us to simultaneously study, in the whole tumor, the relationship between ^{177}Lu distribution, as a surrogate for

absorbed dose, and one aspect of the radiobiological response of the tumor, DNA double strand break damage repair, as measured by γH2AX expression. On average over the whole tumor, ^{111}In-anti-γH2AX-TAT uptake in tumors is increased after ^{177}Lu-DOTATATE therapy over 72 h, similar to our *in vitro* immunofluorescence results. Most interestingly however, within each tumor, the amount of DNA damage, as measured by γH2AX foci, is not strictly correlated with the amount of ^{177}Lu deposition within tumors (Figs. 3 and 5). This suggests a more complex relationship between the amount of ^{177}Lu uptake and the macroscopic radiation deposited dose in various parts of the tumor, with the resulting biological effects, such as DNA damage repair.

This proof-of-principle study shows that DNA damage from MRT can be measured non-invasively, and could potentially be used as an *in vivo* biodosimeter. To the best of our knowledge, this is the first study of this kind, which measures the direct, mechanistic, biological effects of MRT. Understandably, some challenges need to be overcome before translation to the clinic is possible. Our initial results here have been obtained using rat xenograft-bearing athymic mice, but the results can be readily extrapolated to the human situation, given that similar interplay between ^{177}Lu uptake, heterogeneous ^{177}Lu tumor uptake, and DNA damage and repair exists. Without underestimating the importance of the physical radiation deposited dose in tumor and normal tissue for all MRT agents, the radiobiological effects of MRT need to be taken into account when predicting therapeutic outcome. Different tumors react differently to EBRT, as demonstrated in the limited panel of six tumor cell lines. The cell line panel used here also portrays differences in γH2AX kinetics after EBRT, given their different inherent radiosensitivity, and potential further dissimilarities in cell signaling, due to mutations, epigenetic or posttranslational variations in DNA damage repair proteins, and differential stress responses. Therefore, the same must be true for MRT. In addition, MRT effects will be complicated by the combination of receptor expression levels, radionuclide uptake, radionuclide deposited dose, intratumoral heterogeneity (*11*), subcellular distribution (*29*), (radio)biological effects, but also tumor microenvironmental parameters such as hypoxia , and system-wide effects including immune-system effects. Here, we have not considered the effects of those system-wide consequences. As it is used here, ^{111}In-anti-γH2AX-TAT provides one potential biodosimeter to establish a measurement of the radiobiological effects of MRT with ^{177}Lu-DOTATATE. It's clinical applicability is yet to be tested. It is worth noting that γH2AX, and therefore imaging with ^{111}In-anti- γH2AX-TAT, remains a secondary biomarker, and γH2AX can also be upregulated as a result of some other cellular stress responses, such as oncogenic stress, increased genomic instability, and late-stage apoptosis (*18,30*). Therefore, ^{111}In-anti-γH2AX-TAT imaging may not reflect DNA double strand break damage only. The most likely alternative

cause of γH2AX upregulation is MRT-induced apoptosis, resulting in pan-nuclear γH2AX staining. However, we did not observe this in the time span we imaged γH2AX here, making ^{111}In-anti-γH2AX-TAT a suitable agent for imaging the early DNA damage response.

In this work, we show imaging of DNA damage after ^{177}Lu therapy based on a DOTATATE vector, but the same system could be used to evaluate other MRT agents, such as ^{177}Lu-PSMA which is increasingly used for the treatment of prostate cancer, long-range beta-emitting radiopharmaceuticals based on ^{90}Y or ^{131}I, or targeted alpha-emitter therapy based on ^{225}Ac or ^{231}Bi, given their propensity to cause complex DNA damage and abundant γH2AX signals (*31*). γH2AX has also been suggested as a biomarker of normal tissue toxicity, such as renal toxicity following MRT (*32*), and a marker of peripheral blood lymphocyte toxicity (*33*). However, we did not observe any significant changes in renal uptake of ^{111}In-anti-γH2AX-TAT, likely the amount of ^{177}Lu-DOTATATE used in our studies did not to cause clinically significant renal damage, or the physiological renal uptake of ^{111}In-anti-γH2AX-TAT (5.1 ± 0.4%ID/g at 72 h post administration in animals not exposed to ^{177}Lu-DOTATATE) prevents to observe these differences.

Therapy response imaging agents such as ^{111}In-anti-γH2AX-TAT, or its PET alternative ^{89}Zr-anti-γH2AX-TAT (*15*), could find applications in adaptive therapy. Similar to measuring the genotoxic effects of chemotherapy (*17*), external beam radiotherapy (*13*), and radiosensitizers (*16*), measuring the effects of radionuclide therapy *in vivo* may allow adjustment of the therapeutic regimen in accordance to the individual patient's response to that treatment. In addition, non-invasive imaging can reveal differential responses in multiple tumors in the same patient, or elucidate the heterogeneous biological response within the same tumor. Using therapeutic response assessment with molecular imaging, rapid decisions becomes possible, rather than awaiting anatomical changes that potentially follow later, after successful therapy. It is notable however, that metabolic responses to some of the latest targeted therapies are not necessarily accompanied by anatomically obvious response (*34*). Such stratification, possible after a single cycle of MRT allows for adaptive treatment design (*5*), would permit dose reduction to avoid side effects, assess combination therapies, or, in the absence of any measurable response, suggest palliative options designed towards improving quality of life. Moreover, this may also be a financially prudent strategy, given the high cost of each dose of Lutathera™ USD$47,500).

Conclusion

Imaging of the DNA damage response using ^{111}In-anti-γH2AX-TAT provides unique insight following ^{177}Lu-DOTATATE therapy, and allows the visualization of biological response. This includes intratumoral heterogeneity, but also inter-lesion heterogeneity within the same patient.

Key points

QUESTION: Can the radiolabeled antibody ^{111}In-anti-γH2AX-TAT be used *in vivo* to visualise and quantify the γH2AX foci generated at the sites of double strand DNA breaks caused by ^{177}Lu-DOTATATE therapy?

PERTINENT FINDINGS: The γH2AX foci induced by ^{177}Lu-DOTATATE could be imaged by SPECT *in vivo* using ^{111}In-anti-γH2AX-TAT, and correlated with ex vivo and *in vitro* γH2AX levels. γH2AX expression revealed intratumoral and inter-lesion heterogeneity with ^{177}Lu absorbed dose, suggesting a complex biological response to ^{177}Lu therapy.

IMPLICATIONS FOR PATIENT CARE: ^{111}In-anti-γH2AX-TAT can potentially be used as a biodosimeter for optimizing radionuclide treatments such as ^{177}Lu-DOTATATE, both in preclinical investigations and for the design of personalized, adaptive treatment regimes in patients.

REFERENCES

1. Oronsky B, Ma PC, Morgensztern D, Carter CA. Nothing but NET: A review of neuroendocrine tumors and carcinomas. Neoplasia. 2017;19:991-1002.
2. Nicolas GP, Morgenstern A, Schottelius M, Fani M. New developments in peptide receptor radionuclide therapy. J Nucl Med. 2019;60:167-171.
3. Andersson M, Johansson L, Eckerman K, Mattsson S. IDAC-Dose 2.1, an internal dosimetry program for diagnostic nuclear medicine based on the ICRP adult reference voxel phantoms. EJNMMI Res. 2017;7:88.
4. Strosberg J, El-Haddad G, Wolin E, et al. Phase 3 Trial of (177)Lu-dotatate for midgut neuroendocrine tumors. N Engl J Med. 2017;376:125-135.
5. Terry SY, Nonnekens N, Aerts A, et al. Call to arms: need for radiobiology in molecular radionuclide therapy. Eur J Nucl Med Mol Imaging. 2019;46:1588-1590.
6. Bergsma H, Konijnenberg MW, van der Zwan WA, et al. Nephrotoxicity after PRRT with (177)Lu-DOTA-octreotate. Eur J Nucl Med Mol Imaging. 2016;43:1802-1811.
7. Bodei L, Pepe G, Paganelli G. Peptide receptor radionuclide therapy (PRRT) of neuroendocrine tumors with somatostatin analogues. Eur Rev Med Pharmacol Sci. 2010;14:347-351.
8. Kratochwil C, Fendler WP, Eiber M, et al. EANM procedure guidelines for radionuclide therapy with (177)Lu-labelled PSMA-ligands ((177)Lu-PSMA-RLT). Eur J Nucl Med Mol Imaging. 2019;in press
9. Hope TA, Abbott A, Colucci K, et al. NANETS/SNMMI procedure standard for somatostatin receptor-based peptide receptor radionuclide therapy with (177)Lu-DOTATATE. J Nucl Med. 2019;60:937- 943.
10. Del Prete M, Buteau FA, Arsenault F, et al. Personalized (177)Lu-octreotate peptide receptor radionuclide therapy of neuroendocrine tumours: initial results from the P-PRRT trial. Eur J Nucl Med Mol Imaging. 2019;46:728-742.
11. Falzone N, Lee BQ, Able S, et al. Targeting micrometastases: the effect of heterogeneous radionuclide distribution on tumor control probability. J Nucl Med. 2018;60:250-258
12. Knight JC, Koustoulidou S, Cornelissen B. Imaging the DNA damage response with PET and SPECT. Eur J Nucl Med Mol Imaging. 2017;44:1065-1078.
13. Cornelissen B, Kersemans V, Darbar S, et al. Imaging DNA damage in vivo using gammaH2AX-targeted immunoconjugates. Cancer Res. 2011;71:4539-4549.
14. Cornelissen B, Waller A, Able S, Vallis KA. Molecular radiotherapy using cleavable radioimmunoconjugates that target EGFR and gammaH2AX. Mol Cancer Ther. 2013;12:2472-2482.

15. Knight JC, Topping C, Mosley M, et al. PET imaging of DNA damage using (89)Zr-labelled anti-gammaH2AX-TAT immunoconjugates. Eur J Nucl Med Mol Imaging. 2015;42:1707-1717.
16. Fokas E, Prevo R, Pollard JR, et al. Targeting ATR in vivo using the novel inhibitor VE-822 results in selective sensitization of pancreatic tumors to radiation. Cell Death Dis. 2012;3:e441.
17. Knight JC, Mosley MJ, Bravo LC, et al. (89)Zr-anti-gammaH2AX-TAT but not (18)F-FDG allows early monitoring of response to chemotherapy in a mouse model of pancreatic ductal adenocarcinoma. Clin Cancer Res. 2017;23:6498-6504.
18. Cornelissen B, Able S, Kartsonaki C, et al. Imaging DNA damage allows detection of preneoplasia in the BALB-neuT model of breast cancer. J Nucl Med. 2014;55:2026-2031.
19. Kwekkeboom DJ, Bakker WH, Kooij PP, et al. [177Lu-DOTAOTyr3]octreotate: comparison with [111In-DTPAo]octreotide in patients. Eur J Nucl Med. 2001;28:1319-1325.
20. Cornelissen B, Darbar S, Kersemans V, et al. Amplification of DNA damage by a gammaH2AX- targeted radiopharmaceutical. Nucl Med Biol. 2012;39:1142-1151.
21. Boon Quan L, Elliot MA, Sarah A, et al. Radiosensitivity of colorectal cancer to ^{90}Y and the radiobiological implications for radioembolisation therapy. Physics in Medicine & Biology. 2019.
22. Nonnekens J, van Kranenburg M, Beerens CE, et al. Potentiation of peptide receptor radionuclide therapy by the PARP inhibitor olaparib. Theranostics. 2016;6:1821-1832.
23. Dalm SU, Nonnekens J, Doeswijk GN, et al. Comparison of the therapeutic response to treatment with a 177Lu-labeled somatostatin receptor agonist and antagonist in preclinical models. J Nucl Med. 2016;57:260-265.
24. Bol K, Haeck JC, Groen HC, et al. Can DCE-MRI explain the heterogeneity in radiopeptide uptake imaged by SPECT in a pancreatic neuroendocrine tumor model? PLOS ONE. 2013;8:e77076.
25. Melis M, de Swart J, de Visser M, et al. Dynamic and static small-animal SPECT in rats for monitoring renal function after 177Lu-labeled Tyr3-octreotate radionuclide therapy. J Nucl Med. 2010;51:1962-1968.
26. Knight J, Mosley M, Kersemans V, et al. Dual-isotope imaging allows in vivo immunohistochemistry using radiolabelled antibodies in tumours. Nucl Med Biol. 2019;70:14-22.
27. Svensson J, Hagmarker L, Magnander T, Wangberg B, Bernhardt P. Radiation exposure of the spleen during (177)Lu-DOTATATE treatment and its correlation with haematological toxicity and spleen volume. EJNMMI Phys. 2016;3:15.
28. Banath JP, Klokov D, MacPhail SH, Banuelos CA, Olive PL. Residual gammaH2AX foci as an indication of lethal DNA lesions. BMC Cancer. 2010;10:4.

29. Santoro L, Boutaleb S, Garambois V, et al. Noninternalizing monoclonal antibodies are suitable candidates for 125I radioimmunotherapy of small-volume peritoneal carcinomatosis. J Nucl Med. 2009;50:2033-2041.
30. Shah K, Cornelissen B, Kiltie AE, Vallis KA. Can gammaH2AX be used to personalise cancer treatment? Curr Mol Med. 2013;13:1591-1602.
31. Morgenstern A, Apostolidis C, Kratochwil C, Sathekge M, Krolicki L, Bruchertseifer F. An Overview of Targeted Alpha Therapy with (225)Actinium and (213)Bismuth. Curr Radiopharm. 2018;11:200- 208.
32. Pellegrini G, Siwowska K, Haller S, et al. A short-term biological indicator for long-term kidney damage after radionuclide therapy in mice. Pharmaceuticals (Basel). 2017;10:57
33. Denoyer D, Lobachevsky P, Jackson P, Thompson M, Martin OA, Hicks RJ. Analysis of 177Lu-DOTA-octreotate therapy-induced DNA damage in peripheral blood lymphocytes of patients with neuroendocrine tumors. J Nucl Med. 2015;56:505-511.
34. Challapalli A, Aboagye EO. Positron emission tomography imaging of tumor cell metabolism and application to therapy response monitoring. Front Oncol. 2016;6:44.

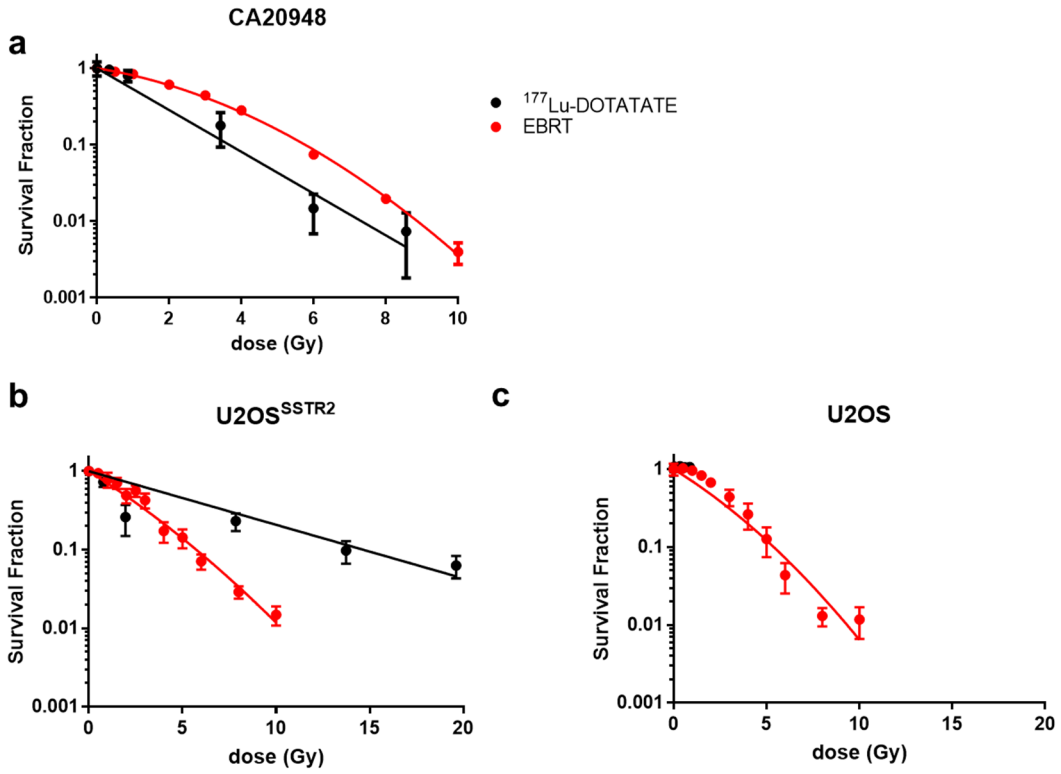

Figure 1: Clonogenic survival following *in vitro* exposure of cancer cell lines to varying amounts of ^{177}Lu-DOTATATE, or increasing amounts of external beam radiation therapy of **(a)** CA20948 cells, **(b)** U2OS^{sstr2} cells, or **(c)** wild type U2OS cells. Radiation absorbed doses for ^{177}Lu were determined based on ^{177}Lu uptake data obtained separately (Supplemental Fig. 4).

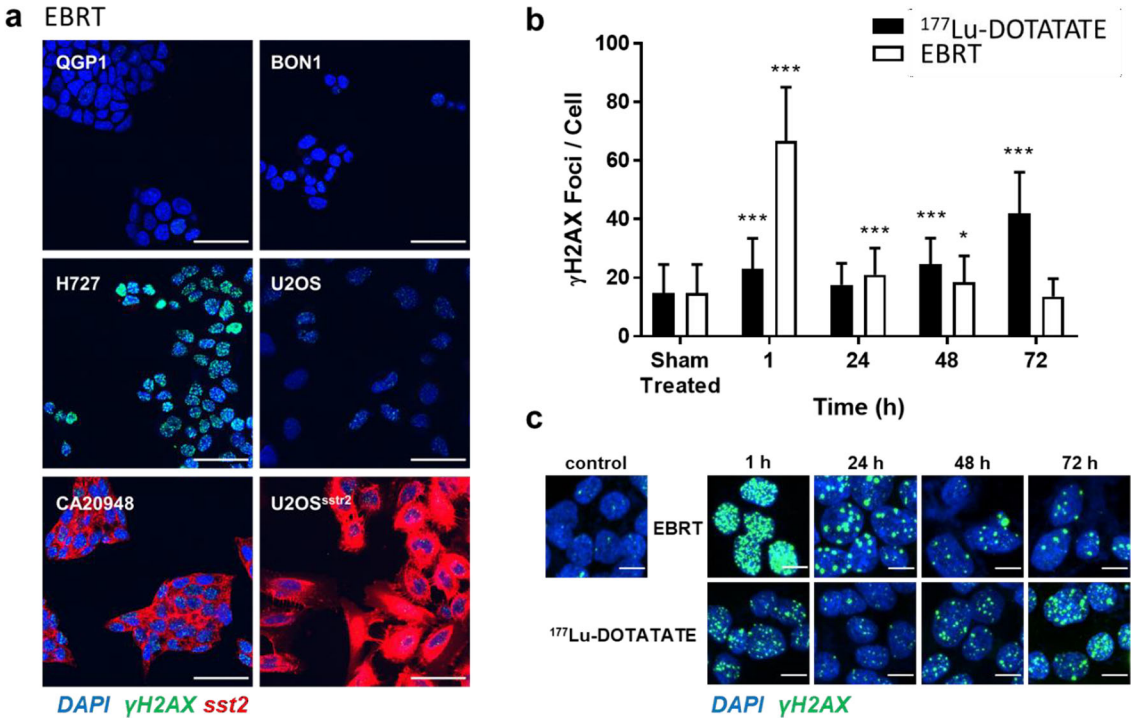

Figure 2: γH2AX foci formation in a panel of cell lines. **(a)** Cells were stained for γH2AX (green) and SST2 (red), one hour after exposure to 4 Gy EBRT. DAPI was used to stain cell nuclei (blue) (scale bar = 50 µm). **(b)** The number of γH2AX foci per cell was determined at various intervals after exposure of CA20948 cells to ^{177}Lu-DOTATATE for 2 h, or after EBRT (6 Gy) (*: P<0.01, ***: P<0.0001). **(c)** Representative immunocytochemistry micrographs (γH2AX = green, nuclei = blue) (scale bar = 10 µm).

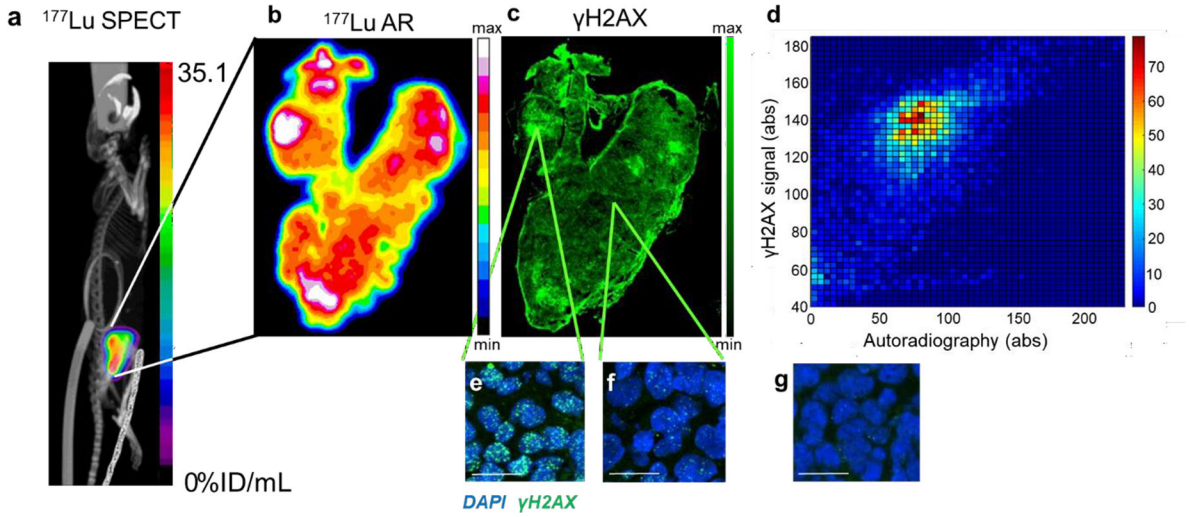

***Figure 3*: (a)** Representative SPECT/CT image, 72 h after intravenous administration of ^{177}Lu- DOTATATE (20 MBq, 0.33 µg) in a CA20948 xenograft-bearing athymic mouse. **(b)** Autoradiography (AR) performed on a tumor section harvested from the same mouse. **(c)** An adjacent section was stained for γH2AX, and the resulting fluorescence micrograph was co-registered to the AR image. (scale bar = 800 µm) **(d)** Density scatterplot based on a pixel-by-pixel analysis of γH2AX signal versus autoradiography (omitting the edge effects on the immunohistochemistry). **(e,f)** High-resolution details of immunohistochemistry in (c), demonstrating γH2AX foci in areas of intense or minimal staining (γH2AX = green; nuclei = blue; scale bar = 20 µm). **(g)** Immunohistochemistry for γH2AX on a representative tumor section from a mouse that was treated with vehicle control only.

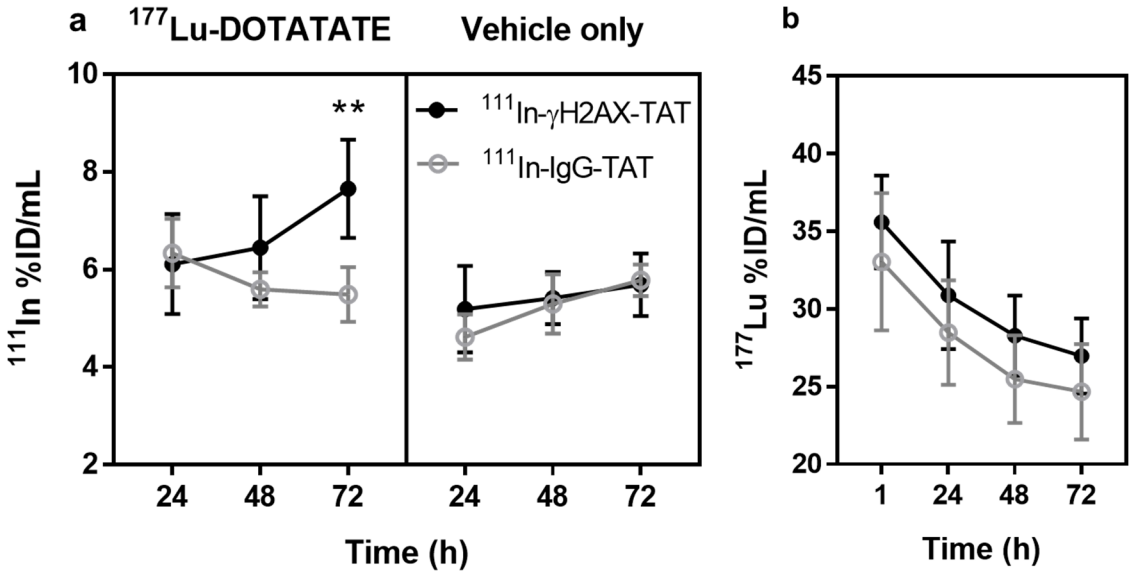

***Figure 4*: (a)** Tumor uptake of ^{111}In-anti-γH2AX-TAT or ^{111}In-IgG-TAT at various times after treatment of CA20948-bearing mice with ^{177}Lu-DOTATATE (20 MBq, 0.33 µg), or vehicle control (**: P<0.005). **(b)** Uptake of ^{177}Lu in the tumor of ^{177}Lu-DOTATATE -treated animals.

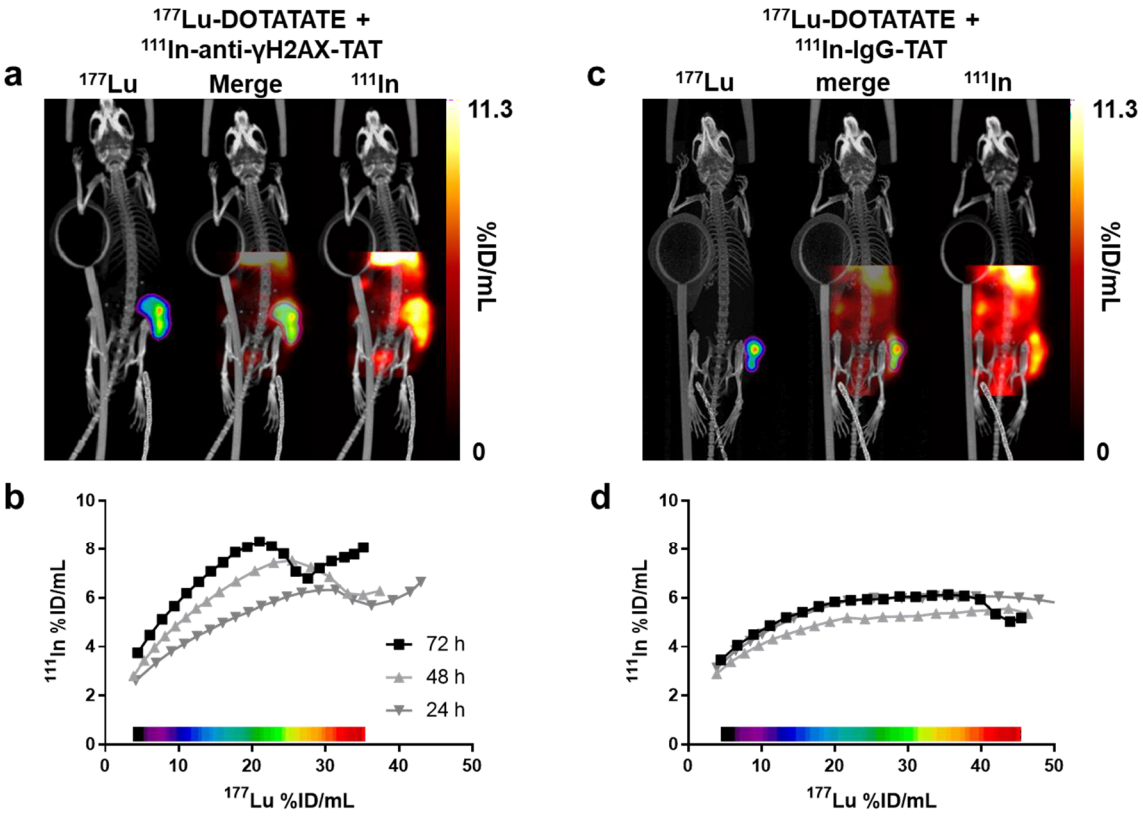

***Figure 5*: (a)** Representative dual isotope SPECT/CT images of mice 71 h after intravenous administration of ^{111}In-anti-γH2AX-TAT (5 MBq, 5 µg), and 72 h after administration of intravenous ^{177}Lu-DOTATATE (20 MBq. 0.33 µg). The tumor is indicated by the purple contour in the ^{177}Lu image.

(b) Correlation between ^{111}In and ^{177}Lu signal in the tumor volume, in voxel collections based on ^{177}Lu signal quantification, based on the SPECT image of the animal in (a). **(c)** Representative dual isotope SPECT/CT images of mice after administration of ^{111}In-IgG-TAT (5 MBq, 5 µg), and ^{177}Lu-DOTATATE (20 MBq. 0.33 µg). The tumor is indicated by the purple contour in the ^{177}Lu image. **(d)** Correlation between ^{111}In and ^{177}Lu signal in the tumor volume, in voxel collections based on ^{177}Lu signal quantification, based on the SPECT image of the animal in (c).

Supplementary material for

Imaging DNA Damage Repair *in vivo* Following ^{177}Lu-DOTATATE Therapy

Edward O'Neill[1], Veerle Kersemans[1], P. Danny Allen[1], Samantha Y.A. Terry[2], Julia Baguña Torres[1], Michael Mosley[1], Sean Smart[1], Boon Quan Lee[1], Nadia Falzone[1], Katherine A. Vallis[1], Mark W. Konijnenberg[3], Marion de Jong[3], Julie Nonnekens[3,4,5], Bart Cornelissen[1,*]

[1] CRUK/MRC Oxford Institute for Radiation Oncology, Department of Oncology, University of Oxford, Oxford, UK
[2] Department of Imaging Chemistry and Biology, King's College London, London, UK
[3] Department of Radiology and Nuclear Medicine, Erasmus MC, Rotterdam, The Netherlands
[4] Department of Molecular Genetics, Erasmus MC, Rotterdam, The Netherlands
[5] Oncode Institute, Erasmus MC, Rotterdam, The Netherlands

Supplementary Materials and Methods

General

All reagents were purchased from Sigma-Aldrich unless otherwise stated and were used without further purification. The chelating agent *p*-SCN-Bn-DTPA was purchased from Macrocyclics Inc. (Dallas, TX). Water was deionised using a Barnstead NANOpure purification system (Thermo Scientific) and had a resistance of >18.2 MΩ/cm at 25°C. Protein concentration measurements were made using a ND-1000 spectrophotometer (NanoDrop Technologies, Inc.). Instant thin-layer chromatography (iTLC) was performed with glass microfiber chromatography paper (Agilent Technologies) and strips were analysed with a Bioscan AR-2000 radio-TLC scanner (Eckert & Ziegler). pH was determined using pH indicator paper (Merck Millipore). Radioactivity measurements were made using a CRC-25R dose calibrator (Capintec, Inc.).

Cells

Six cancer cell lines were used, incorporating cells with high and low expression levels of SST2, and to compensate for possible defects in DNA damage response signaling in one of the cell lines. The neuroendocrine cancer patient-derived BON1, QGP1, and H727 cells express low levels of SST2. BON1 (derived from a human enterochromaffin cell serotonin-producing pancreatic neuroendocrine tumor) was kindly provided by Professor Simona Glasberg from Hadassah-Hebrew University Medical Center and maintained in 1:1 DMEM/Ham's F-12. QGP1 (human pancreatic somatostatinoma) was obtained from the Japanese Collection of Research Bioresources Cell Bank (JCRB) and maintained in RPMI 1640. H727 (human lung neuroendocrine carcinoma) obtained from the American Type Culture Collection was maintained in RPMI 1640. U2OS cells were obtained from ATCC, whereas U2OS cells transfected to stably express high SST2 levels ($U2OS^{sstr2}$) were generated at Erasmus MC (*1*). Both U2OS variants were maintained in DMEM. CA20948 cells, a rat pancreatic neuroendocrine cancer cell line that overexpresses SST2, were originally derived from solid tumor tissue at Erasmus MC, and maintained in Dulbecco's Modified Eagle Medium (DMEM) supplemented with 1 mM sodium pyruvate (*2*). All cells were supplemented with 10% fetal bovine serum (FBS), 2 mM L-glutamine, 100 units/mL penicillin, and 0.1 mg/mL streptomycin. Cells were grown in a 37°C environment containing 5% CO_2 and were harvested and passaged as required using trypsin-EDTA solution. Cells were authenticated by the provider and regularly tested for the absence of mycoplasma contamination. The cumulative length of culture was less than 6 months following retrieval from liquid nitrogen storage.

Cell uptake and cell fractionation

Cell membrane-association, internalization and nuclear localisation of ^{177}Lu-DOTATATE were studied in CA20948, BON1, QGP1, H727, U2OS and $U2OS^{SSTR2}$ cell lines. Radiolabelled ^{177}Lu-DOTATATE (2.5 MBq/mL, 50 MBq/nmol) was added to aliquots of 2×10^5 cells, previously detached using Accutase (Biolegend Inc), in 200 µL of their respective growth media in 1.5 mL tubes at 37°C. The samples were gently agitated by a rocking plate inside the incubator. All samples were centrifuged at 500×g for 2 min, and culture medium was removed. The cells were resuspended in ice-cold PBS (pH 7.4) and centrifuged again. The PBS was removed, combined with the previously separated medium and counted in a γ-counter to measure cell-free radioactivity. Cell-surface bound material was removed by resuspension of the cells in 500 µL of glycine buffer (0.1 M glycine.HCl, pH 2.5) for 6 min on ice (*3*). Samples were centrifuged at 500×g for 2

min, the supernatant containing the membrane-bound fraction was removed, and cells washed twice with PBS and combined with the fractions containing glycine buffer. Cell pellets were then resuspended in 500 µL of cell membrane lysis buffer (25 mM KCl, 5 mM $MgCl_2$, 10 mM Tris-HCl and 0.5% NP-40). After incubation on ice for 6 min, the lysate was centrifuged at 1000×g for 2 min to separate cytoplasm-associated ^{177}Lu (supernatant) from the nuclear-associated content. The nuclear fraction was washed with 500 µl of lysis buffer, the suspension was recentrifuged and the supernatant was removed and combined with that previously separated. Radioactivity in the membrane, cytoplasmic and nuclear fractions was measured using an automated gammacounter (*3,4*).

***In vitro* immunofluorescence**

Cells grown in 8-well chambered cell culture slides, 10,000 in a total volume of 200 µL cell culture medium (Falcon), were exposed to ^{177}Lu-DOTATATE (2.5 MBq/mL, 50 MBq/nmol) and incubated at 37°C in 5% CO_2 for 2 h; or exposed to external irradiation (6 Gy); or sham treated/irradiated. Cells were then washed with PBS, provided with fresh growth media, and left to recover for 1, 24, 48, or 72 h at 37°C in 5% CO_2. After recovery, cells were washed with PBS and fixed using 4% paraformaldehyde solution for 10 min. After washing, the cells were permeabilised using 0.2% triton X-100 in TBS buffer (50 mM Tris-Cl, pH 7.5. 150 mM NaCl) for 10 min at room temperature, and briefly rinsed with TBS. Non-specific binding was blocked with 2% BSA in TBST (0.1% Tween-20/TBS) for 1 h at room temperature. Primary antibody (mouse anti γH2AX Millipore, Clone JBW-301, 1:800) diluted in blocking buffer was applied directly on the slide and incubated overnight at 4°C, and then washed with TBST. Fluorescently labelled secondary antibody, dylight-488 goat anti-mouse (Invitrogen A11034, 1:250 in blocking buffer) was applied and incubated for 1 h at room temperature. After further washing with PBS, slides were mounted using Vectashield containing DAPI to visualise cell nuclei (Vector Labs). Images were acquired on an Andor Dragonfly microscope (Oxford Instruments), using a 40x/1.3 oil lens to generate a series of z-stacks.

***In vitro* Microdosimetry**

The total radiation absorbed dose from ^{177}Lu to cell nuclei was determined using a MIRD-based approach. The total dose was calculated as the sum of self-dose and cross-dose.

Cell dimensions: Determination of S-values for dosimetry depends on cell dimensions. These were measured by fluorescence microscopy. Live cells were detached using accutase (Biolegend), washed with PBS, incubated with Hoechst 33342 (Abcam) and CellBrite Orange cytoplasmic membrane dye (Insight

Biotechnology) for 15 min at 37°C, then embedded in low melting point agarose (Trevigen), and deposited on a microscope slide with a glass coverslip for immediate imaging. The average spherical dimensions of the cell membrane and nucleus for each cell type were calculated from the average of the length x width of the membrane and nucleus in the central plane of each suspended cell from z-stacks of fluorescence images collected using a Leica SP8 fluorescence microscope (Leica), using a 63x/1.4 oil lens.

Self-dose: Dose-point kernels (DPKs) were calculated with the general-purpose Monte Carlo code PENELOPE (*5*) using the complete electron spectrum of ^{117}Lu based on the unabridged β^- spectrum from MIRD RADTABS (*6*) and the spectrum of conversion, Auger and Coster-Kronig electrons from *BrIccEmis* (*7*), determined by means of event-by-event simulation as previously described (*8*). Photon dose was omitted due to the low intensity and small geometry. A total of $1x10^8$ primary particles were simulated in each run with a statistical uncertainty $\leq$ 0.4% achieved in each bin of a 1-nm-thick spherical water shell. Assuming a cell model of two concentric homogenous spheres of liquid water (mass density ρ = 1 gcm^{-3}), representing the cell and its nucleus and taking the nucleus as the target, absorbed fractions per decay (self-dose *S*-values) were calculated from the simulated DPKs to determine contributions from the nucleus (N←N), the cytoplasm (N←Cy) or the cell surface (N←CS).

Cross-dose: Two geometries representing cells in suspension (first 2 hours) and cells plated (the following 2 weeks) were considered. For the cells in suspension, a target cell is immersed in a spherical water medium of 2 mm in radius (33.5 µL). This particular radius is chosen as the continuous-slowing-down-approximation (CSDA) range of the most energetic β^- electrons (E_{max,β^-} = 498 keV) in water is about 1.7 mm. Radioactivity was assumed to be uniformly distributed throughout the water medium but outside the target cell. For the plated cells, a target cell is placed on the base and at the centre of a well of 1.75 cm radius. The well is filled with water of 2.08 mm depth (2 mL). In order to achieve similar levels of statistical uncertainty compared with the case of cells in suspension, a cuboid water medium of 4 mm in length and width and 2.08 mm in height (33.3 µL) surrounding the target cell was used as the source volume. A total of $1x10^8$ primary particles were simulated in each run. Cross-dose *S*-values was determined from the energy deposited in the target cell nucleus by the radioactivity distributed uniformly in the source volume.

Total self-dose to each cell was determined by the product of self-dose *S*-values and cumulative decays from different cell compartments calculated using trapezoidal integration for the first 2 hours using uptake data and assuming purely physical decays after that. Total cross-dose was similarly calculated by

using cross-dose *S*-values and only considering cumulative decays from the environment as a result of physical decay.

SPECT/CT Imaging

SPECT/CT images were acquired using a VECTor^{4}CT scanner (MILabs, Utrecht, The Netherlands) equipped with a HE-UHR-RM collimator containing pinhole apertures of 1.8 mm diameter. The scanner was calibrated during each imaging session by imaging a phantom with either an indium-111 or lutetium-177 standard solution. Data were acquired in list mode (gamma spectrum collection from 0-1200 keV) using MILabs acquisition software v7.15. Triple-energy-window based scatter correction was applied for the indium-111 photon peaks (155.7-188 and 228-271.7 keV) and background peaks (148.8-155.7, 187.3-192.2, 225.4-228.3 and 271.7-282.6 keV) and lutetium-177 peaks (103-126 and 197-221 keV) and background peaks (98.4-103, 126-130.6, 192.2-197 and 221-225 keV). All images were reconstructed with MILabs reconstruction software v3.24 to 0.6 mm isotropic 3D voxel grids using dual matrix similarity regulated ordered-subset expectation maximisation (dual matrix SROSEM, using 4 iterations and 2 subsets for lutetium-177 and 4 subsets for indium-111). Subsequently, whole body CT images were acquired at 50 kV and 0.24 mA using continuous rotation (40 degrees/s). After reconstruction, the SPECT and corresponding CT data were co-registered and re-sampled to equivalent 200 µm isotropic voxels. CT-based attenuation correction was applied.

Reconstructed images were viewed and analysed using PMOD v.3.38 (PMOD Technologies, Zurich, Switzerland). Tumour uptake of indium-111 for lutetium-177 treated mice was calculated based upon VOIs generated by the segmentation tool in PMOD, which represented CT-based volumes that contained magnitudes equal and greater than 20%ID/mL of lutetium-177. . A spherical VOI with the same volume was used to calculate tumour uptake of indium-111 in mice that did not receive ^{177}Lu-DOTATATE. Results were reported as percentage of the injected dose per mL of tissue (%ID/mL).

***In Vivo* Studies**

All animal procedures were performed in accordance with the UK Animals (Scientific Procedures) Act 1986 and with local ethical committee approval. For ^{177}Lu-DOTATATE biodistribution studies, xenograft tumours were established in the right hind flank of female athymic BALB/c *nu/nu* mice (Charles River) by subcutaneous injection of CA20948 (5×10^6 cells), or QGP1 (1×10^7 cells), or BON1 (5×10^6 cells), or H727 (5×10^6 cells) in sterile PBS (100 µL). When tumours reached a diameter of approximately 10 mm, ^{177}Lu-

DOTATATE (20 MBq, 0.33 µg) in sterile PBS (100 µL) was injected intravenously *via* the lateral tail vein. SPECT/CT images were acquired at 1 h and the next day either at 16 h or 24 h after injection, including one mouse undergoing dynamic acquisition after injection using 5 min frames. After the final imaging session, mice were euthanised by cervical dislocation and selected organs, tissues and blood were removed and transferred into pre-weighed counting tubes. The weight of and amount of radioactivity in each was measured using a HiDex gamma counter (Lablogic). Counts were converted into radioactivity units (MBq) using a calibration curve generated from known standards. All values were decay-corrected to the time of injection, and the percentage of the injected dose per gram (%ID/g) of each sample was calculated. Five animals were used per group. Flash-frozen xenograft tissue from mice was cyrosectioned (to 10 µm sections) and analysed by autoradiography using a Cyclone Plus Phosphor Imager (PerkinElmer). Adjacent *ex vivo* tissue sections were probed by immunofluorescence for γH2AX foci formation and compared with xenograft tissue obtained from treatment-naive mice.

In a separate study, CA20948 subcutaneous xenografts were established in the right hind flank of female athymic BALB/c *nu/nu* mice as above. Xenograft-bearing mice were administered ^{177}Lu-DOTATATE (20 MBq, 0.33 µg) in sterile PBS (100 µL), or PBS only, by intravenous injection *via* the lateral tail vein. SPECT/CT images were acquired at 1, 24, 48, 72 h post ^{177}Lu-DOTATATE injection. In addition, mice were administered ^{111}In-anti-γH2AX-TAT (5 MBq, 5 µg), or ^{111}In-IgG-TAT (5 MBq, 5 µg) in sterile PBS (100 µL) injected intravenously immediately after the 1 h imaging session *via* the lateral tail vein (see scheme below). After the final imaging session, mice were euthanised by cervical dislocation and selected organs, tissues and blood were removed and transferred into pre-weighed counting tubes with radioactivity spectra measured using a HiDex automated gamma counter. Activities for each isotope were calculated from area under curve analysis using GraphPad prism, based upon standard curves of mixtures containing known activities of lutetium-177 and indium-111. All values were decay-corrected to the time of injection, and the percentage of the injected dose per gram (%ID/g) of each sample was calculated. Five animals were used per group.

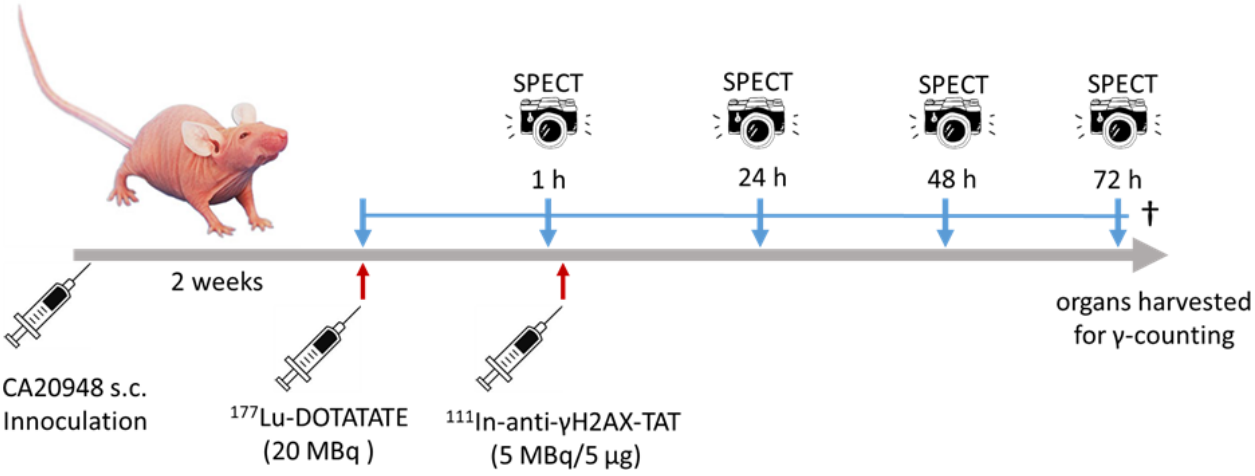

Supplemental Fig. 1: Schematic representation of the therapy and imaging protocol.

***In vivo* ^{177}Lu dosimetry**

The absorbed doses in the tumour xenografts by ^{177}Lu-DOTATATE were determined by using the spheres dosimetry S-values from the IDAC code (*9*). The absorbed dose rate at each time-point was calculated by multiplying the activity at that time-point with the ^{177}Lu S-value interpolated according to their initial volume, assuming a mass density of 1.03 g/cm^3 (lympatic nodes). The tumour time-activity data were fitted with a single exponential curve using Graphpad prism. At each imaging time-point the absorbed dose was calculated by integrating the exponential time-activity curve from time of injection (t=0) to the imaging time-point to obtain the cumulative activities as well as to infinity. Following the MIRD-scheme the absorbed dose is the product of the cumulated activity and the S-value.

***Ex vivo* immunofluorescence and autoradiography**

Sections of tumour xenograft were obtained at 10 µm thickness using a cryostat (CM1950, Leica Biosystems). Tissue sections were allowed to reach room temperature and were then washed in PBS and fixed using 4% paraformaldehyde solution for 10 min. After washing, the sections were permeabilised with 0.2% triton/TBS for 10 min at room temperature, washed again with TBS and blocked in 2% BSA in TBST with glycine 0.3 M and 5% goat serum for 1 h in a flat humid chamber at room temperature. Primary anti-γH2AX antibody (JBW301, Millipore), diluted (1:800) in blocking buffer (minus glycine) was applied directly to the slide and incubated in a humid chamber at 4°C overnight, and then washed with TBST. Fluorescently labelled secondary antibody, 1:250 dilution of a goat anti-rabbit IgG Alexa Fluor® 488 (Invitrogen A11034) was applied directly to the slide and incubated in a humid chamber at room

temperature for 1 h. After further washing, excess fluid was removed and a small drop of Vectashield plus DAPI (Vector H-1200) was applied to each section and a coverslip placed on the slide and secured with Covergrip (Biotium 23005). Fluorescence micrographs were acquired on an Andor Dragonfly microscope (Oxford Instruments) using a 40x/1.3 oil lens. Autoradiography was performed on adjacent sections, using a digital autoradiography platform (Cyclone, Perkin Elmer). Micrographs were registered to autoradiographs using a landmark-based MATLAB algorithm developed in-house. Coincidence of anti-γH2AX antibody associated fluorescence with autoradiography signal was performed on binned co-registered adjacent slides using rigid registration with the JaCOP (Just Another Co-localisation Plugin) in ImageJ.

Supplementary Tables

Supplemental Table 1: Estimated α and β values for linear quadratic equations fitted to clonogenic survival curves in a panel of six cell lines after either exposure to increasing doses of ^{177}Lu-DOTATATE for 2 h, or EBRT. Since clonogenic survival of U2OS, QGP-1, BON-1 and H727 were not significantly affected by ^{177}Lu-DOTATATE (plating efficiency >90%), α and βg values could not be calculated.

cell line	EBRT	^{177}Lu-DOTATATE
CA20948	α = 0.18 ± 0.01, β = 0.038 ± 0.001	α = 0.63 ± 0.07, $\beta g < 10^{-6}$
U2OS	α = 0.34 ± 0.04, β = 0.017 ± 0.005	NA
U2OS^{SSTR2}	α = 0.34 ± 0.02, β = 0.01 ± 0.002	α = 0.16 ± 0.03, $\beta g < 10^{-6}$
QGP1	α = 0.18 ± 0.01, β = 0.0063 ± 0.0007	NA
BON1	α = 0.32 ± 0.02, β = 0.017 ± 0.003	NA
H727	α = 0.06 ± 0.01, β = 0.027 ± 0.001	NA

Supplemental Table 2: Accumulated absorbed radiation dose from ^{177}Lu in tumour tissue, after administration of ^{177}Lu-DOTATATE (20 MBq, 0.33 μg) in CA20948-tumour-bearing mice.

IDAC	**Absorbed dose (Gy)**									
	^{177}Lu-DOTATATE / ^{111}In-IgG-TAT					**^{177}Lu-DOTATATE / ^{111}In-anti-γH2AX-TAT**				
Time (h)	m1	m2	m3	m4	m5	m6	m7	m8	m9	m10
1	0.27	0.36	0.24	0.22	0.33	0.38	0.26	0.28	0.24	0.31
24	5.5	7.5	4.6	4.4	6.8	8.1	5.0	5.7	4.7	6.5
48	9.5	13.0	7.7	7.3	11.6	14.2	8.0	9.8	7.5	11.2
72	12.3	17.0	9.7	9.3	15.1	18.8	9.8	12.8	9.3	14.6
infinity	19.4	28.1	13.4	13.1	24.2	32.8	12.5	20.4	12.0	23.9

Supplemental Figures

Supplemental Fig. 2: $^{111}In/^{177}Lu$ dual SPECT imaging using the MILabs VECtor^{4} small animal SPECT/CT scanner, of a series of 1.5 mL tubes filled with 50-250 kBq or ^{177}Lu and 50 kBq of ^{111}In.

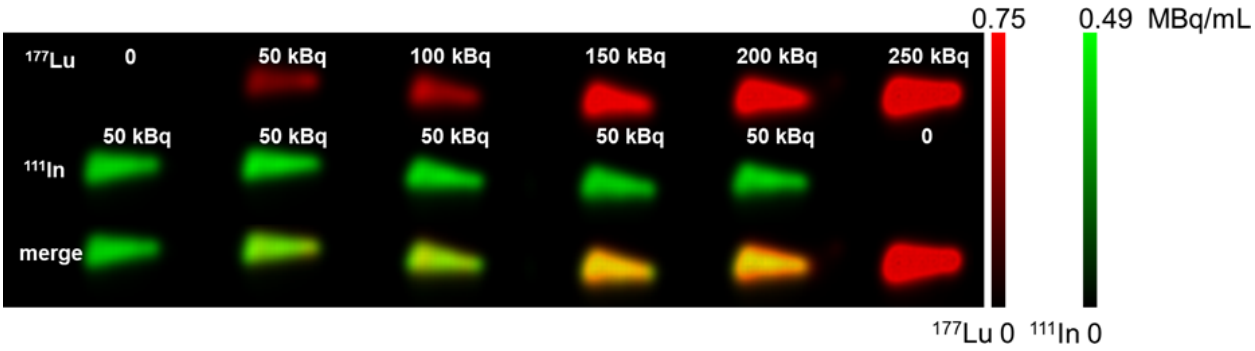

Supplemental Fig. 3: Clonogenic survival following *in vitro* exposure of cancer cell lines to varying amounts of ^{177}Lu-DOTATATE, or increasing amounts of external beam radiation therapy. **(a)** QGP1 cells, **(b)** BON1 cells, or **(c)** H727 cells. Radiation absorbed doses for ^{177}Lu were determined based on ^{177}Lu uptake data obtained from a separate study (Supplementary Figure S3).

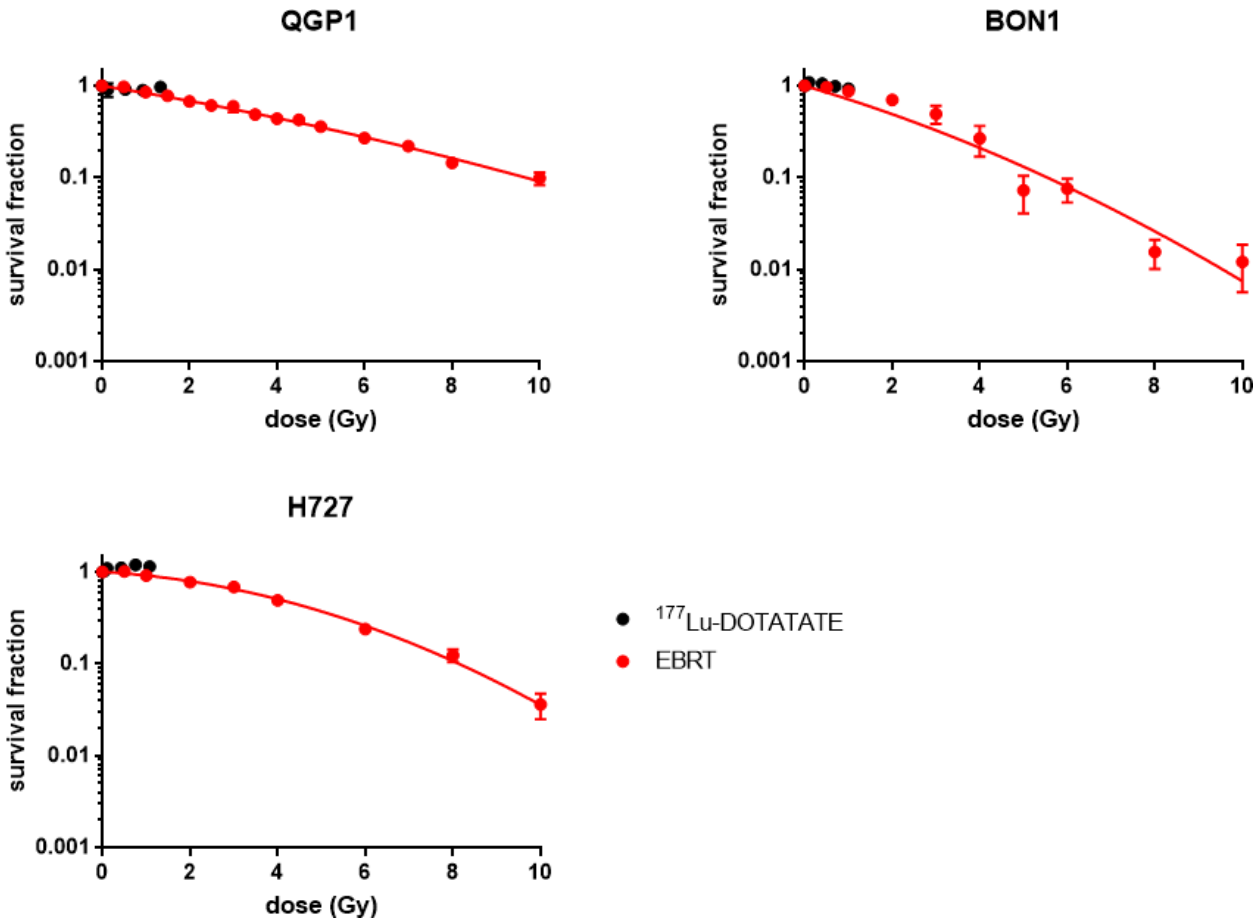

Supplemental Fig. 4: *In vitro* uptake of ^{177}Lu-DOTATATE in a panel of cell lines. Aliquots of 2×10^5 cells were exposed to ^{177}Lu-DOTATATE (2.5 MBq/mL, 50 MBq/nmol, in 200 µL) for up to 24 h at 37°C. The amount of ^{177}Lu associated with the cell membrane, cytoplasm and cell nuclei was determined after cell fractionation. Please note the difference in Y-axis scales.

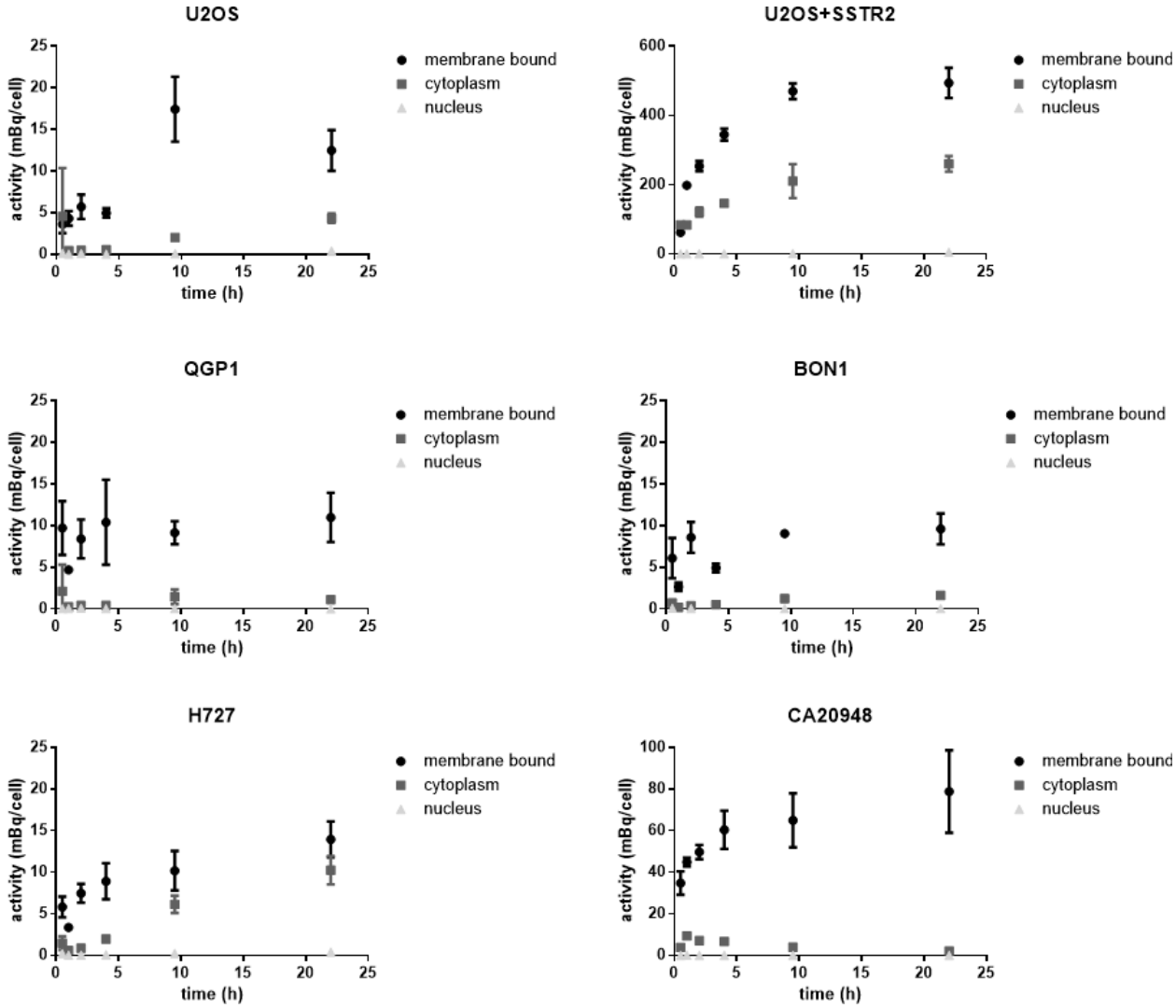

Supplemental Fig. 5: The number of γH2AX foci per cell was determined at various intervals after exposure of U2OS^{sstr2} or wild type U2OS cells to ^{177}Lu-DOTATATE for 2 h, or after EBRT (6 Gy).

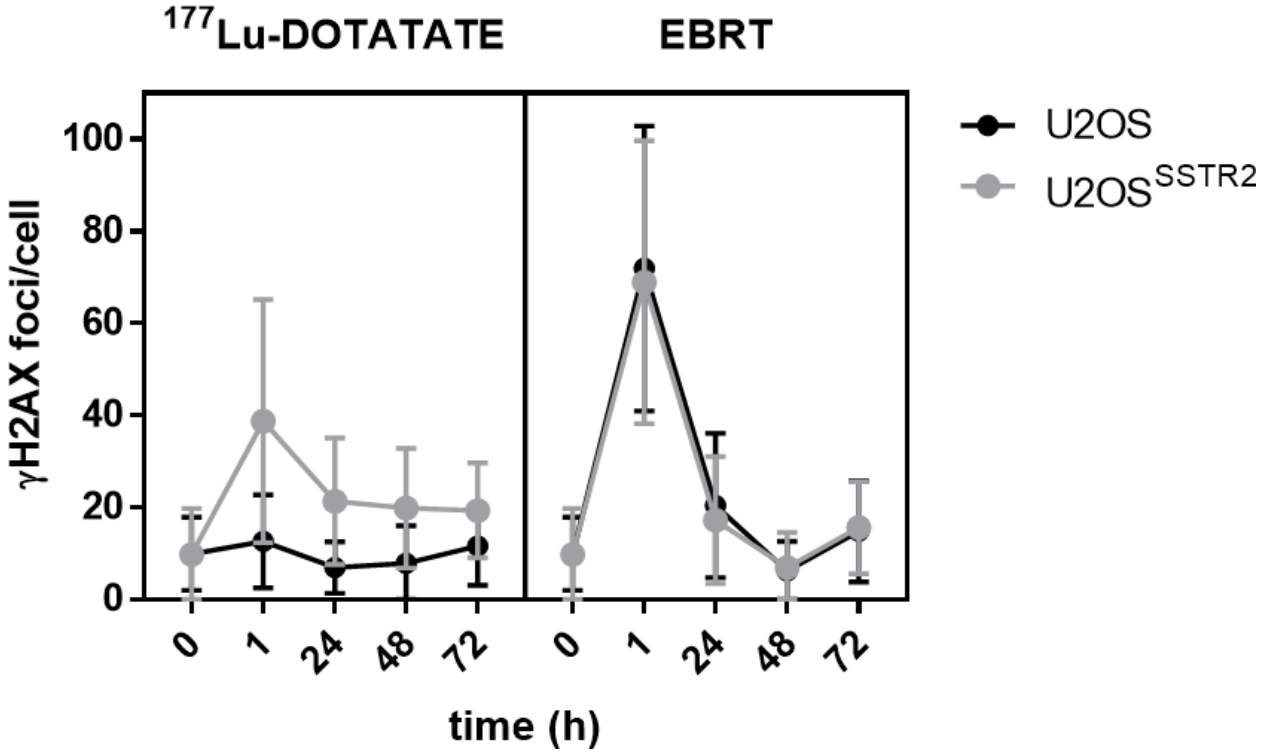

Supplemental Fig. 6: (a) Distribution of ^{177}Lu in tumour, blood and selected tissues, 24 h after intravenous administration of ^{177}Lu-DOTATATE (20 MBq, 0.33 µg) to mice bearing QGP1, H727, BON1, or CA20948 xenograft tumours (n = 5). **(b)** Representative VOI analysis of dynamic SPECT imaging of ^{177}Lu uptake in a CA20948 tumour xenograft within the first 110 min after administration.

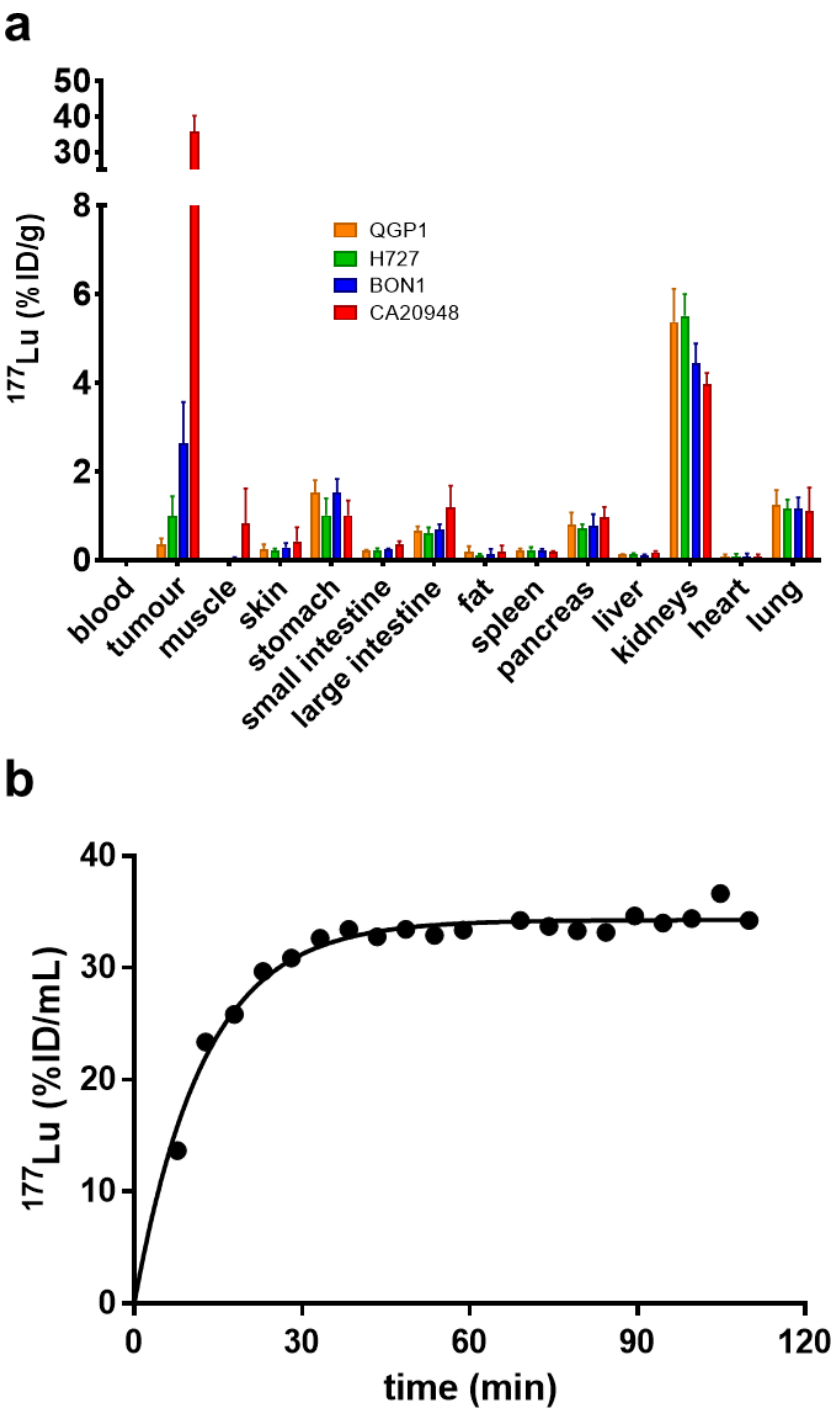

Supplemental Fig. 7: Representative Autoradiography of ^{177}Lu and γH2AX immunohistochemistry of tumour xenograft sections harvested, 72 h after intravenous administration of ^{177}Lu-DOTATATE (20 MBq, 0.33 µg) in a CA20948 xenograft-bearing athymic mouse. As in Fig. 3A and 3C. Three additional examples of ^{177}Lu-DOTATATE uptake in tumour sections, correlated with γH2AX expression. (scale bar = 500 µm)

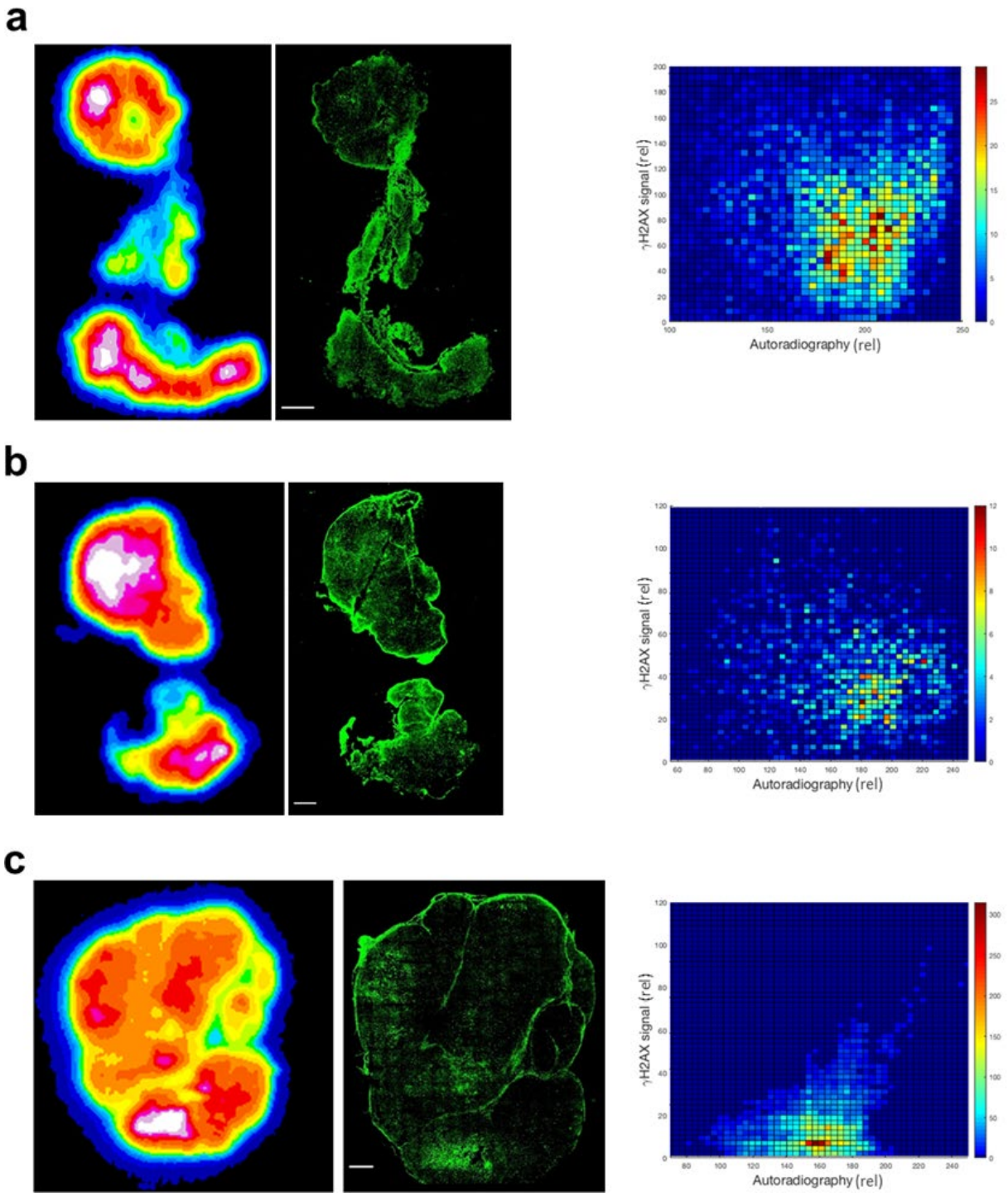

Supplemental Fig. 8: As in Fig. 4A. Tumour uptake in individual mice bearing CA20948 xenografts of ^{111}In-anti-γH2AX-TAT or ^{111}In-IgG-TAT at various times after treatment of mice with ^{177}Lu-DOTATATE (20 MBq, 0.33 µg) **(a)** or vehicle control **(b)**.

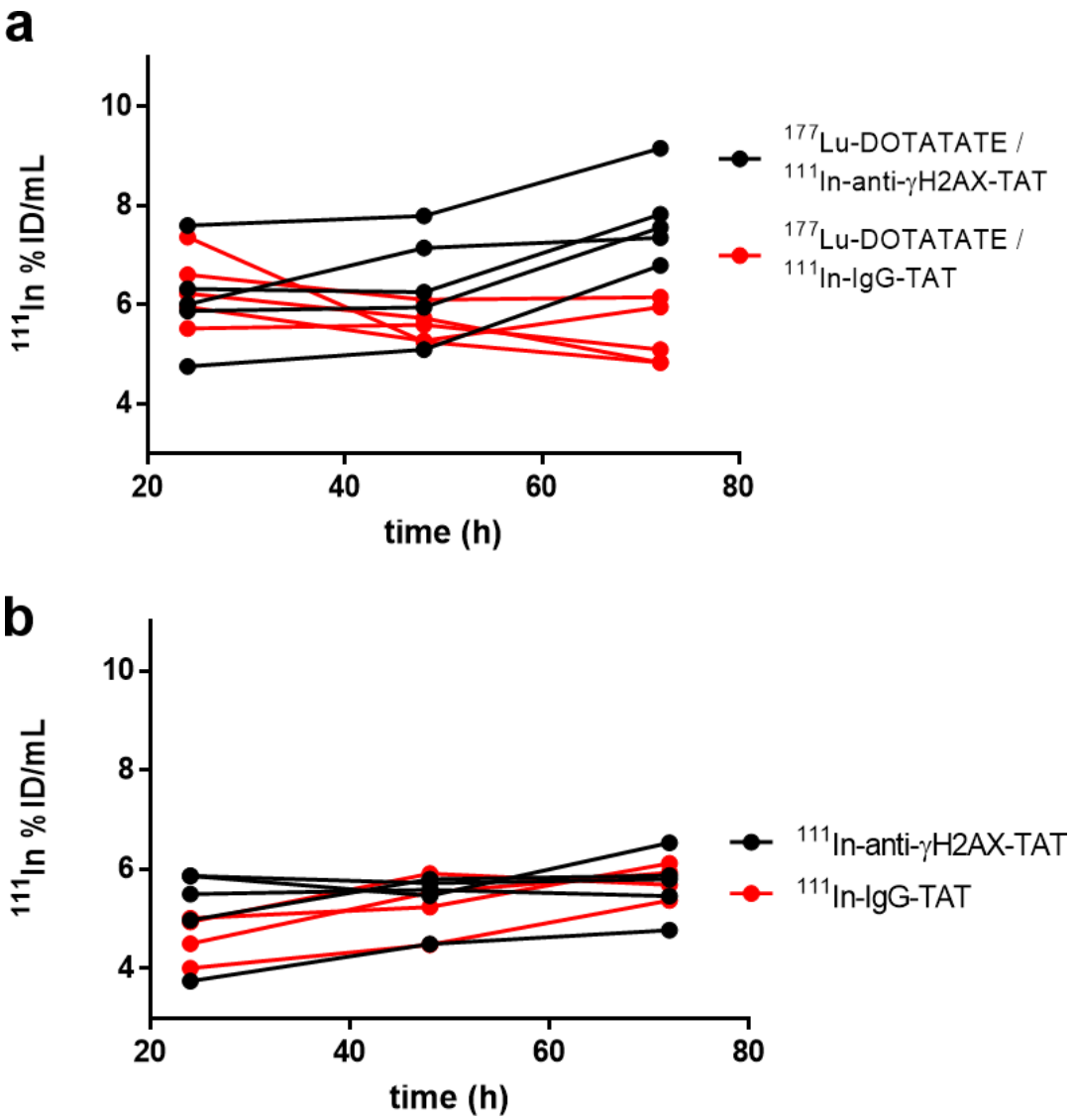

Supplemental Fig. 9: (a) Distribution of ^{111}In in blood and selected tissues, 72 h after intravenous administration of ^{111}In-anti-γH2AX-TAT or ^{111}In-IgG-TAT in mice bearing CA20948 xenografts treated with ^{177}Lu-DOTATATE (20 MBq, 0.33 µg) or vehicle control. **(b)** Distribution of ^{177}Lu in ^{177}Lu-DOTATATE-treated animals.

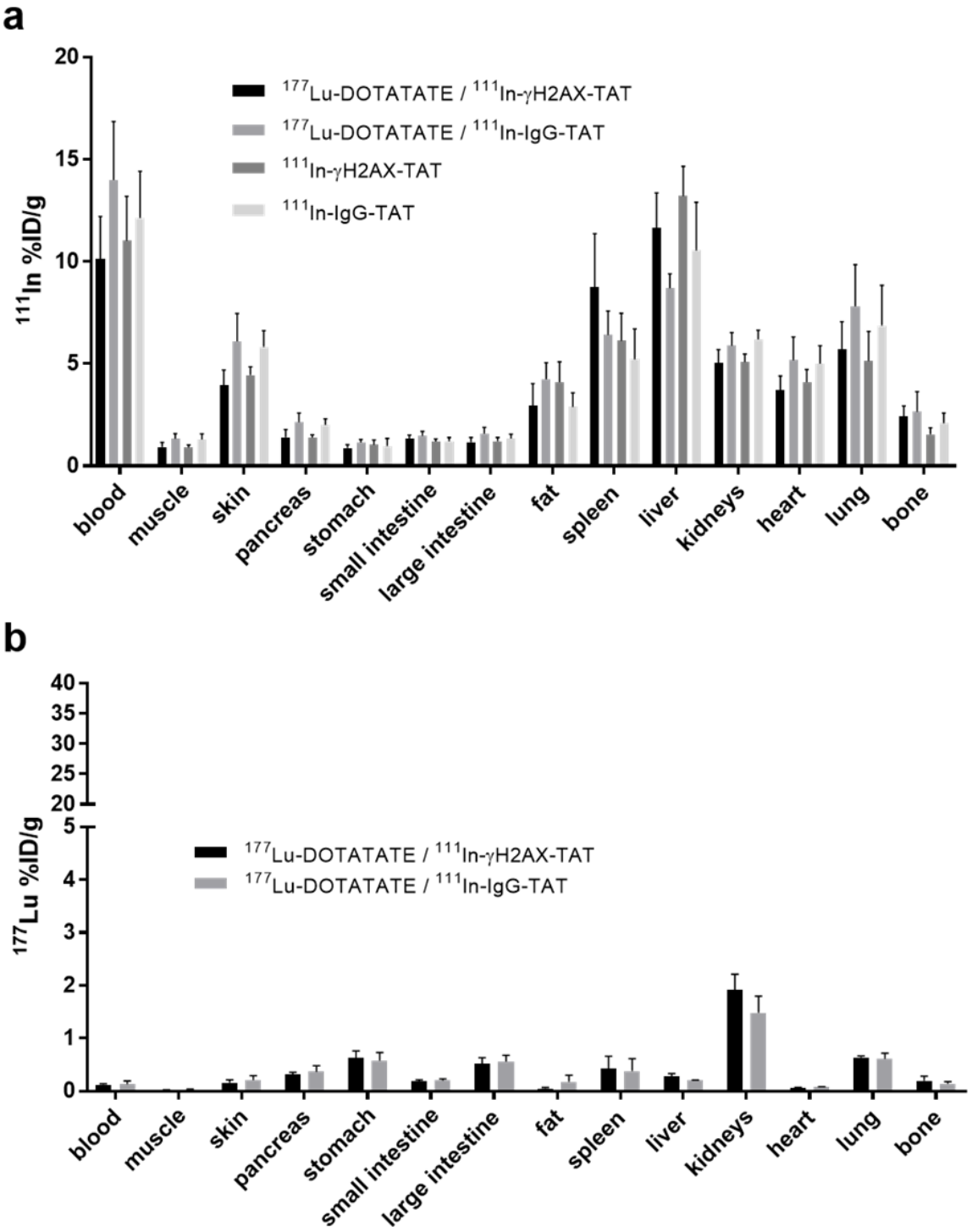

Supplemental Fig. 10: Tumour uptake of ^{177}Lu-DOTATATE time-activity curves, with single exponential curve fits (Pearson $R^2 > 0.94$), the dashed lines indicate the 95% confidence intervals, in mice administered ^{177}Lu-DOTATATE and ^{111}In-IgG-TAT (m1-m5) or ^{177}Lu-DOTATATE and ^{111}In-anti-γH2AX-TAT. S-values for ^{177}Lu were obtained from the spheres model in the IDAC code (lymphatic nodes).

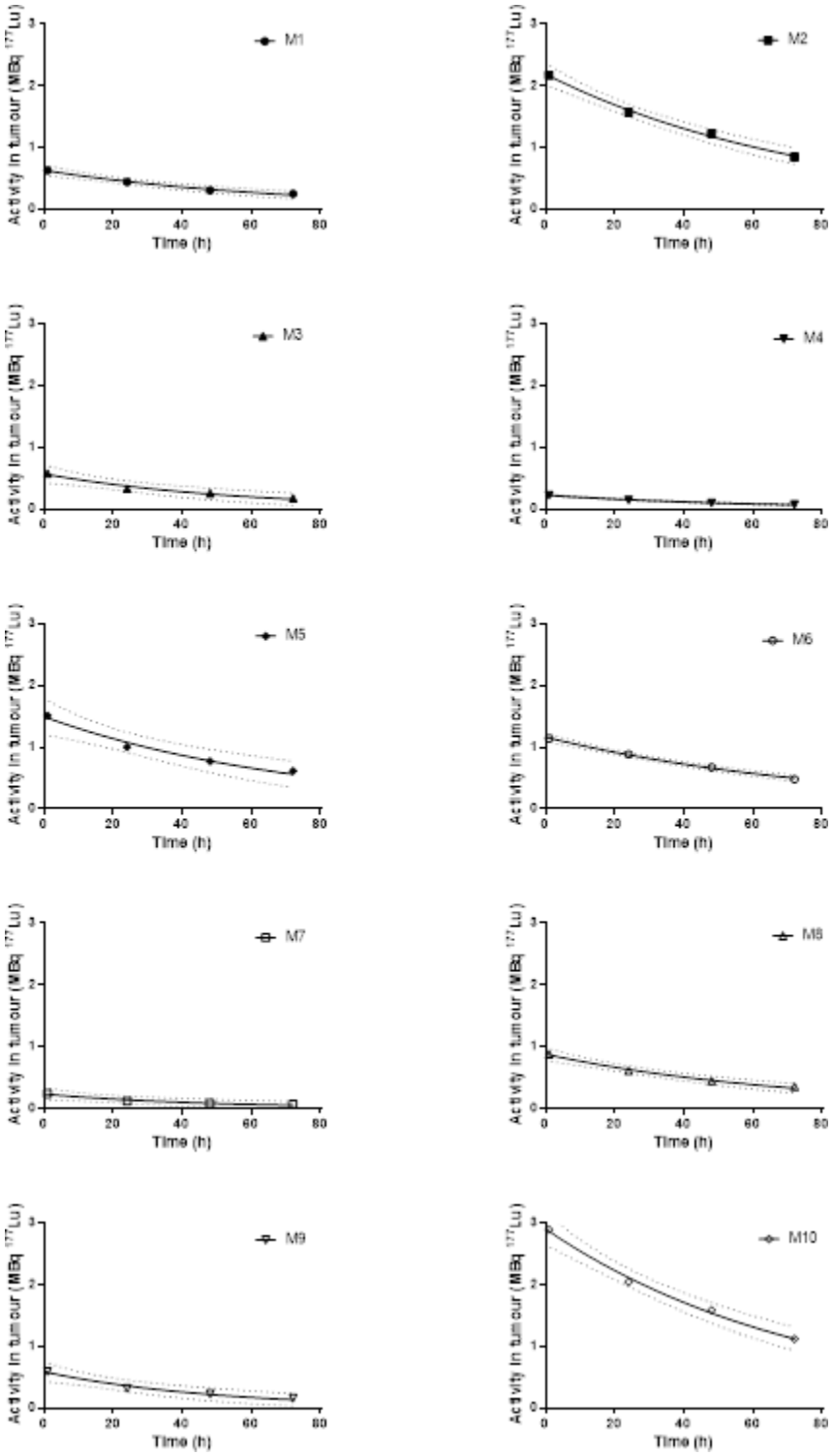

References for Supplementary Material

1. Dalm SU, Nonnekens J, Doeswijk GN, et al. Comparison of the Therapeutic Response to Treatment with a 177Lu-Labeled Somatostatin Receptor Agonist and Antagonist in Preclinical Models. *J Nucl Med.* 2016;57:260-265.

2. Bernard BF, Krenning E, Breeman WA, et al. Use of the rat pancreatic CA20948 cell line for the comparison of radiolabelled peptides for receptor-targeted scintigraphy and radionuclide therapy. *Nucl Med Commun.* 2000;21:1079-1085.

3. Cornelissen B, Hu M, McLarty K, Costantini D, Reilly RM. Cellular penetration and nuclear importation properties of 111In-labeled and 123I-labeled HIV-1 tat peptide immunoconjugates in BT-474 human breast cancer cells. *Nucl Med Biol.* 2007;34:37-46.

4. Goddu SM, Howell RW, Rao DV. Cellular dosimetry: absorbed fractions for monoenergetic electron and alpha particle sources and S-values for radionuclides uniformly distributed in different cell compartments. *J Nucl Med.* 1994;35:303-316.

5. Salvat F, Fernandez-Varea JM, Sempau J. *PENELOPE-2011: A Code System for Monte Carlo Simulation of Electron and Photon Transport*: OECD Nuclear Energy Agency, Issy-les-Moulineaux; 2011.

6. Lee BQ, Nikjoo H, Ekman J, Jonsson P, Stuchbery AE, Kibedi T. A stochastic cascade model for Auger-electron emitting radionuclides. *Int J Radiat Biol.* 2016;92:641-653.

7. Falzone N, Fernandez-Varea JM, Flux G, Vallis KA. Monte Carlo Evaluation of Auger Electron-Emitting Theranostic Radionuclides. *J Nucl Med.* 2015;56:1441-1446.

8. Falzone N, Lee BQ, Able S, et al. Targeting Micrometastases: The Effect of Heterogeneous Radionuclide Distribution on Tumor Control Probability. *J Nucl Med.* 2018.

9. Andersson M, Johansson L, Eckerman K, Mattsson S. IDAC-Dose 2.1, an internal dosimetry program for diagnostic nuclear medicine based on the ICRP adult reference voxel phantoms. *EJNMMI Res.* 2017;7:88.